Master Thesis

THE GEOLOGY OF THE LAUTERBACH GASFIELD

Geologic modelling in a complex depozone

– Leoben, 2010 –

Martin Geißler, BSc

Advisor of the Chair of Petroleum Geology:

Univ.-Prof. Mag.rer.nat. Dr.mont. Reinhard Sachsenhofer

Advisor of RAG:

DI Daniel Pöttler

I declare in lieu of oath, that I wrote this thesis and performed the associated research myself, using only literature cited in this volume.

Leoben, September 2010

Acknowledgements

First of all I would like to thank my supervisor at the University of Leoben, Professor Sachsenhofer, who gave me the opportunity work on this practical oriented topic. He always added valuable ideas to my work with looking at things from a different point of view.

I would like to thank the people from RAG, first of all Daniel Pöttler who made this master thesis possible and supported me whenever I needed information, know-how and motivation. Additionally, I would like to mention Klaus Eder and Wilma Troiss who helped me when I got lost in the complex world of Petrel.

Thanks to the team at the University of Leoben, where Stefan, Gloria, Doris and Jürgen were always there for a valuable discussion and jokes in the coffee break.

I would also like to mention the people of Schlumberger, who enabled the use of Petrel at the University of Leoben with a software grant.

Last but not least I would like to thank my family and my girlfriend Kerstin, who supported me whenever things got complicated.

Table of Contents

Abstract

The Lauterbach Gas Field is located in a wedge top deposition environment resulting in a complex architecture. Therefore, every well drilled delivered new insights and altered the perception of reservoir setting. Thus, the aim of the present master thesis is to build a geologic 3D model that reflects the complexity of the reservoir and fulfils the needs of a dynamic reservoir simulation. A dataset provided by Rohöl-Aufsuchungs AG consisting of 3D seismic data and well data forms the base for this study.

The Lauterbach Basin is a piggyback basin that formed on top of the Molasse Imbrications and is located at the border of Salzburg and Upper Austria. The basin has an extension of approximately 5.5 x 3.5 km and is truncated in the south by the Alpine thrust system. Above the base, formed by a regional erosional event, five productive reservoir layers were deposited. Turbiditic sediments were shed into the basin from SSE directions. In some layers a second input direction from E is identifiable. The key elements in basin history are the synsedimentary stress from the underlying moving Molasse Imbrications that led to soft deformation of the sediments and a large number of erosive events that are represented in the sedimentary succession.

Well log correlation and seismic interpretation in this setting are challenging, because bed thickness is often not much greater than seismic resolution. As a consequence, top and base of a reservoir layer cannot be mapped separately in seismic. According to synthetic seismograms, the reflectors were chosen to represent the top of the reservoir sections. The base of each reservoir successions was constructed using thickness maps that are based on amplitude variations along the seismic reflectors. Furthermore, pressure data from production tests formed a valuable assist in the identification of reservoir connectivity. To characterize the geology of the Lauterbach Basin, a facies model of the reservoir was built using an object based modelling technique. The definition and distribution of different facies groups within the reservoir is essential for the calculation of hydrocarbon volume in place, which was also carried out. The results showed an excellent fit with independent estimates derived from production pressure data.

Kurzfassung

Das Gasfeld Lauterbach wurde in einem „wedge-top“ Ablagerungsraum gebildet. Es zeichnet sich daher durch einen sehr komplexen Aufbau aus. Aus diesem Grund veränderte jede neu abgeteufte Bohrung das Verständnis für die Lagerstätte grundlegend.

Das Ziel dieser Arbeit war es, die komplexe strukturelle und sedimentologische Geschichte des Lautberbach Gasfeldes zu erfassen und in einem statischen geologischen 3D Modell abzubilden. Dieses sollte auch den Anforderungen einer dynamischen Reservoirsimulation genügen. Die Basis für diese Studie bildet ein Datensatz bestehend aus 3D seismischen Daten und Daten von Bohrungen, die von der Rohöl-Aufsuchungs AG zur Verfügung gestellt wurden.

Das Lauterbach Becken ist ein Piggy-back Becken das an der salzburgisch-/oberösterreichischen Grenze liegt und sich über den Molasse Schuppen gebildet hat. Das Becken hat eine Ausdehnung von ca. 5.5 x 3.5 km und wird im Süden durch den Alpenkörper überschoben. Über der Beckenbasis, die durch eine regional verfolgbare Erosionsfläche definiert ist, wurden fünf gasführende Sedimentintervalle abgelagert. Die turbiditischen Sedimente werden hauptsächlich aus Richtung SSE in das Becken eingetragen, in tieferen Intervallen ist auch Sedimenteintrag aus östlicher Richtung erkennbar. Zwei Hauptfaktoren sind bei der Beckenentwicklung maßgebend: synsedimentäre Deformation durch den Druck der unterlagernden Molasse Schuppen und die hohe Anzahl erosiver Ereignisse, die in der Sedimentabfolge erkennbar ist.

Die Log-Korrelation und die Interpretation von seismischen Daten stellten sich als herausfordernd dar, da die Schichtmächtigkeiten oft in der Größenordnung der seismischen Auflösung oder darunter liegen. Aus diesem Grund sind in den seismischen Daten Top und Basis eines Intervalls nicht seperat auflösbar. Auf der Basis von synthetischen Seismogrammen lassen sich die Reflektoren dem Top des zugehörigen Reservoirintervalls zuordnen, die Basis der einzelnen Reservoir Zonen wurde über Mächtigkeitskarten konstruiert. Der Trend in der Mächtigkeitsvariation der Schichtpakete wurde aus der seismischen Amplitude abgeleitet. Weiters bilden Druckdaten aus Tests eine wichtige Hilfestellung in der Identifikation der Konnektivität von einzelnen

Intervallen. Um die komplexe Geologie des Ablagerungsmilieus in einem 3D Modell abbilden zu können, wurde die fazielle Ausbildung der vorliegenden Sedimente in der Modellierung berücksichtigt. Die Charakterisierung und Verteilung der unterschiedlichen Faziesgruppen bildet eine wichtige Grundlage für die abschließende Bestimmung der Kohlenwasserstoffmenge in der Lagerstätte. Die berechneten Volumina zeigeten eine hervoragende Übereinstimmung mit jenen, die unabhängig aus Druckdaten der produzierenden Bohrungen ermittelt wurden.

Introduction & Problem

Approaching complex reservoirs like the Lauterbach Gas Field with a stock tank based understanding of reservoir behaviour is often not sufficient. Reservoir characterisation can be optimized with a deeper understanding of the geologic processes that led to the formation of the reservoir.

The link between geological input and reservoir behaviour can be accomplished with the construction of a 3D geological model. This state of the art technique is used not only to calculate hydrocarbon volumes in the reservoir, but also to reach an understanding of the reservoir framework and the geologic events controlling its formation. This will allow better forecasts for the behaviour of future wells based on the experience of the past.

In this study, the geologic events that led to formation of the Lauterbach Basin and the deposition of the reservoir intervals within the basin will be investigated. In addition, the workflow of how the geologic input is transferred into a geologic 3D reservoir model is explained.

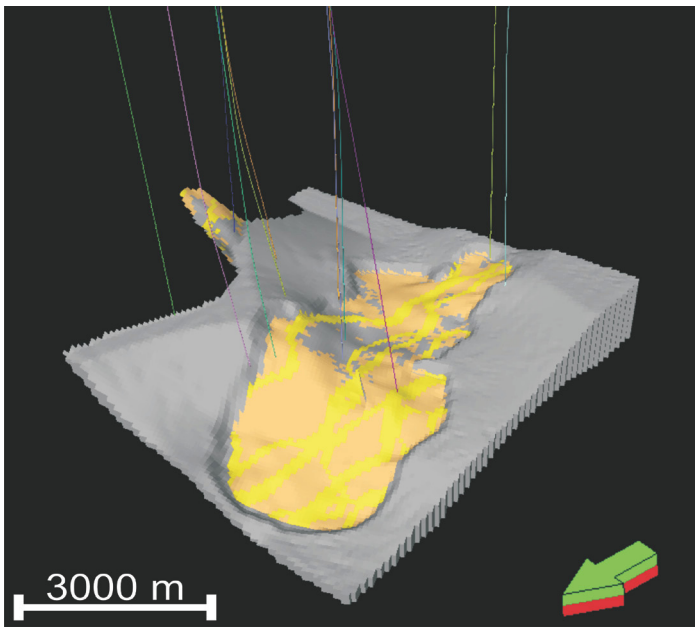

Fig. 1: Static geologic model of the Lauterbach Gas Field in 3D view

Geological Setting

The Austrian Molasse Basin is part of the E – W trending peripheral North Alpine Foreland Basin, which extends from French Savoie in the West to lower Austria in the East over a length of approximately 700 km and width between 20 and 150 km (Sissingh, 1997). In the Austrian part (Salzburg, Upper- and Lower Austria), the northern margin of the basin is formed by the outcropping Bohemian Massif, whereas the southern margin aligns with the Alpine thrust front (Fig. 2). However seismic and well data show that sediments of the Molasse Basin extend underneath the thrust sheets of the Alps (Kollmann, 1977).

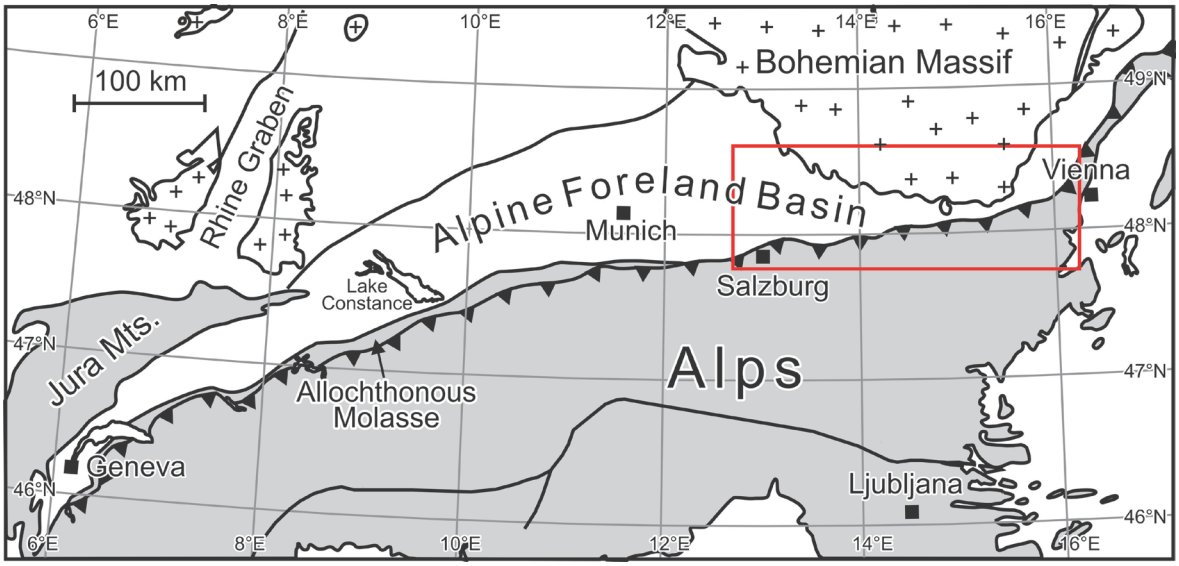

Fig. 2: Location of the Austrian Molasse Basin within the North Alpine foreland Basin

The Molasse sediments of Cenozoic age overlie Variscan basement rocks that are widely covered with Mesozoic sediments. The Cenozoic basin fill reaches a maximum thickness of approximately 5000 m near the thrust front and thins northwards, highlighting the characteristic triangular shaped geometry of peripheral foreland basins (Bachmann, et al., 1986). The Cenozoic sediments are divided into three tectonic units: The undisturbed *Autochthonous Molasse,* the *Allochthonous Molasse* (including Molasse Imbrications, disturbed Molasse and Waschberg Zone) and the *Parautochthonous Molasse*, consisting of Molasse Sediments riding piggyback upon Helveticum, Flysch or East Alpine nappes (Wagner, 1998).

Basin Development, Paleogeography and Sedimentation

The structural evolution of the North Alpine Foreland Basin is strongly linked to the Cenozoic phases of the Alpine orogeny, which is related to the convergence of the Aplulian Microplate and the Eurasiatic Plate due to anticlockwise movement of the African continent (Sissingh, 1997). Four important stages, interrupted by periods of tectonic activity and erosion, can be found in the development of the Molasse Basin and its basement:

1. During Permo-Carboniferous times, graben formation occurred.
2. During Jurassic times, the area was part of the Middle European carbonate platform.
3. In Cretaceous times, the later Molasse basement was part of the northern shelf of the Helvetic Sea. Glauconitic shales and sandstones were deposited.
4. In early Cenozoic times, the collision of the Alps with the shelf of the Eurasiatic plate led to the deformation of the foreland. The Molasse Basin was formed as pelagic foredeep of the Alpine orogenic system (Wagner, 1998).

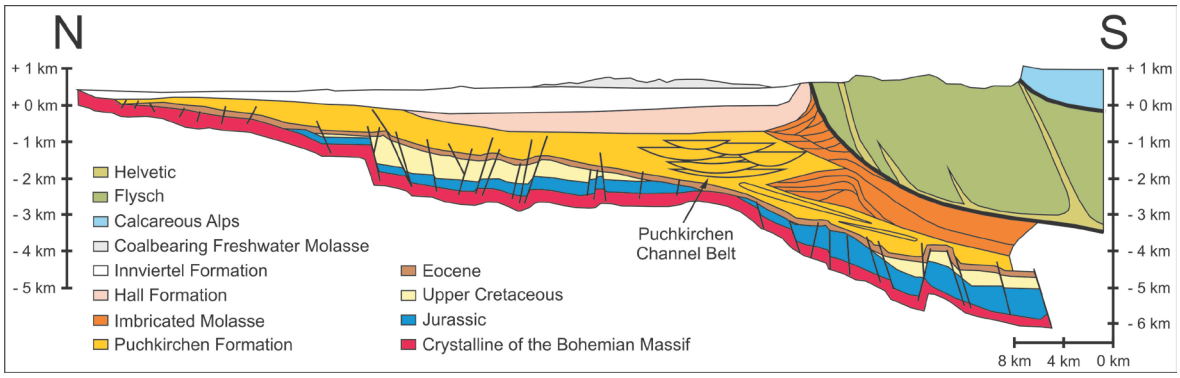

Fig. 3: N – S cross section through the Molasse Basin, modified from Wagner (1996)

Crystalline Basement & Structural Evolution

The Bohemian Massif, part of the Variscian orogenic system of Europe, forms the crystalline basement of the later Molasse Basin. It is composed of medium to high grade metamorphic rocks and Variscian granitic plutonites and bends southward under the Alpine nappes to a depth of 4000 – 8000m. The basement is dissected by a conjugate system of NW-SE and NE-SW trending faults and secondary fault systems running N-S and E-W (Fig. 4), segmenting it into blocks ((Wagner, 1998).

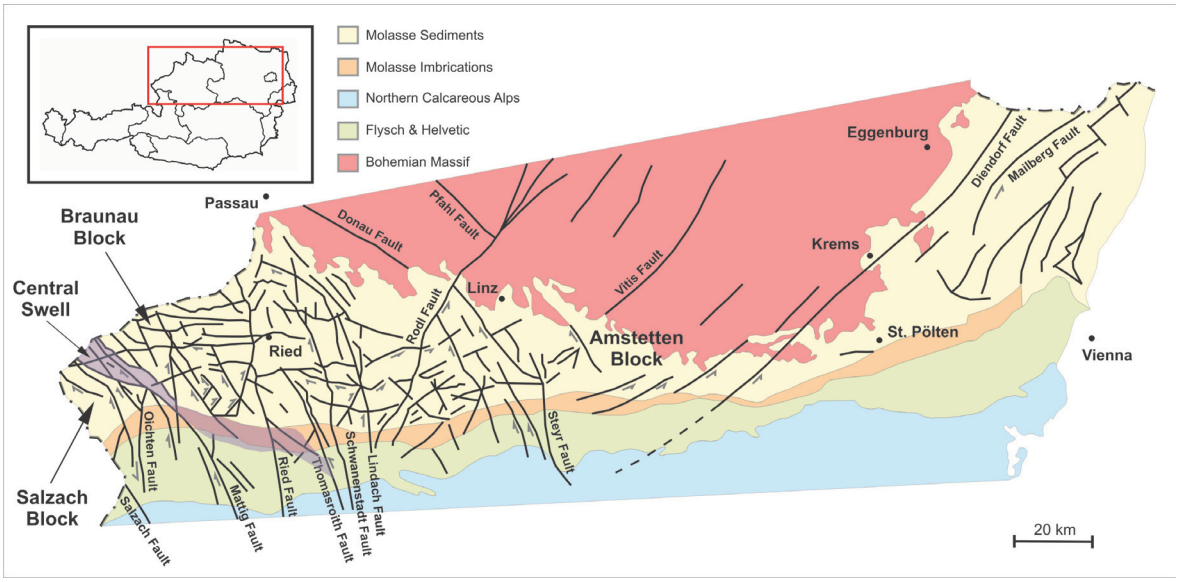

Fig. 4: Faults in the Molasse basement, modified from Wagner (1998)

An important structural feature in the eastern part of the basin is the Central Swell (Fig. 4), a NW-SE trending high, separating the Salzach- and the Braunau-Block. The Amstetten-Block, limited by the major Steyr and Diendorf faults, divides the foreland Molasse between Upper and Lower Austria at the surface. This feature extends approximately 40 km to the south below the Alpine nappes (Malzer, et al., 1993).

The basement of the Molasse Basin was stretched in Mesozoic and Eocene times in a southward direction, resulting in the reactivation of Palaeozoic conjugate NE-SW and NW-SE trending fault systems. During late Eocene – early Oligocene times the European Plate was flexed due to the subduction process and the weight of the advancing Alpine nappes. This led to the formation of E-W trending (basin-parallel) extensional faults, which formed traps for most of the Mesozoic and Cenozoic oil bearing reservoirs in Austria. From Miocene times on almost all faults were integrated in a transpressional stress regime. Locally, soft sediments on top of the competent Eocene rocks started to overthrust at sharp bends of the E-W trending fault pattern and the faults became sealing. The NE and NW trending fault system acted as drainage for the oil migration from below the thrust sheets (Malzer, et al., 1993; Wagner, 1998).

Palaeozoic Setting

Palaeozoic rocks in the Upper Austrian Molasse Basin seem to be limited to graben structures at the south-western margin of the Central Swell. Those Permian-Carboniferous rocks reach a thickness of up to 1000 m and are composed of fluvial sandstone, silts and clays with interbedded coal seams. Although the sediments were dated with spores, there is a fair chance that those spores might have been redeposited from older rocks. In Lower Austria, Sediments of Palaeozoic age (shale, sandstone and breccia) can be found in a Graben structure near Zöbing. No economic hydrocarbon accumulations have been found so far in Palaeozoic rocks in the Austrian Molasse Basin (Malzer, et al., 1993; Wagner, 1998).

Mesozoic Setting

Above the crystalline rocks of the Bohemian Massif and the Palaeozoic strata, Mesozoic sediments (also referred to as *Autochthonous Mesozoic*) are widely distributed in the subsurface of the Molasse Basin (Fig. 5). In contrast to Switzerland and Germany, no Triassic strata are preserved in the Austrian Molasse Basin. Thus, the oldest Mesozoic sediments are dated as Jurassic (Bajocian) (Bachmann, et al., 1986; Wagner, 1998). Starting with coal-bearing fluviatile sands at the base, the setting changed to a shallow marine depositional environment. Shallow marine sandstones are overlain by fossil rich, light grey to brownish limestones and dolomites of the Carbonate Group. The carbonatic evolution continues up to early Cretaceous, where lagoonal dolomites, siliceous limestones and breccia affected by fresh-water complete this succession. Those carbonates form the equivalent to the carbonate platform in southern Germany. The Jurassic sediments reach a thickness of up to 800 m but were completely eroded in the northern and north-eastern part of the basin, as well as on the Central Swell (Malzer, et al., 1993).

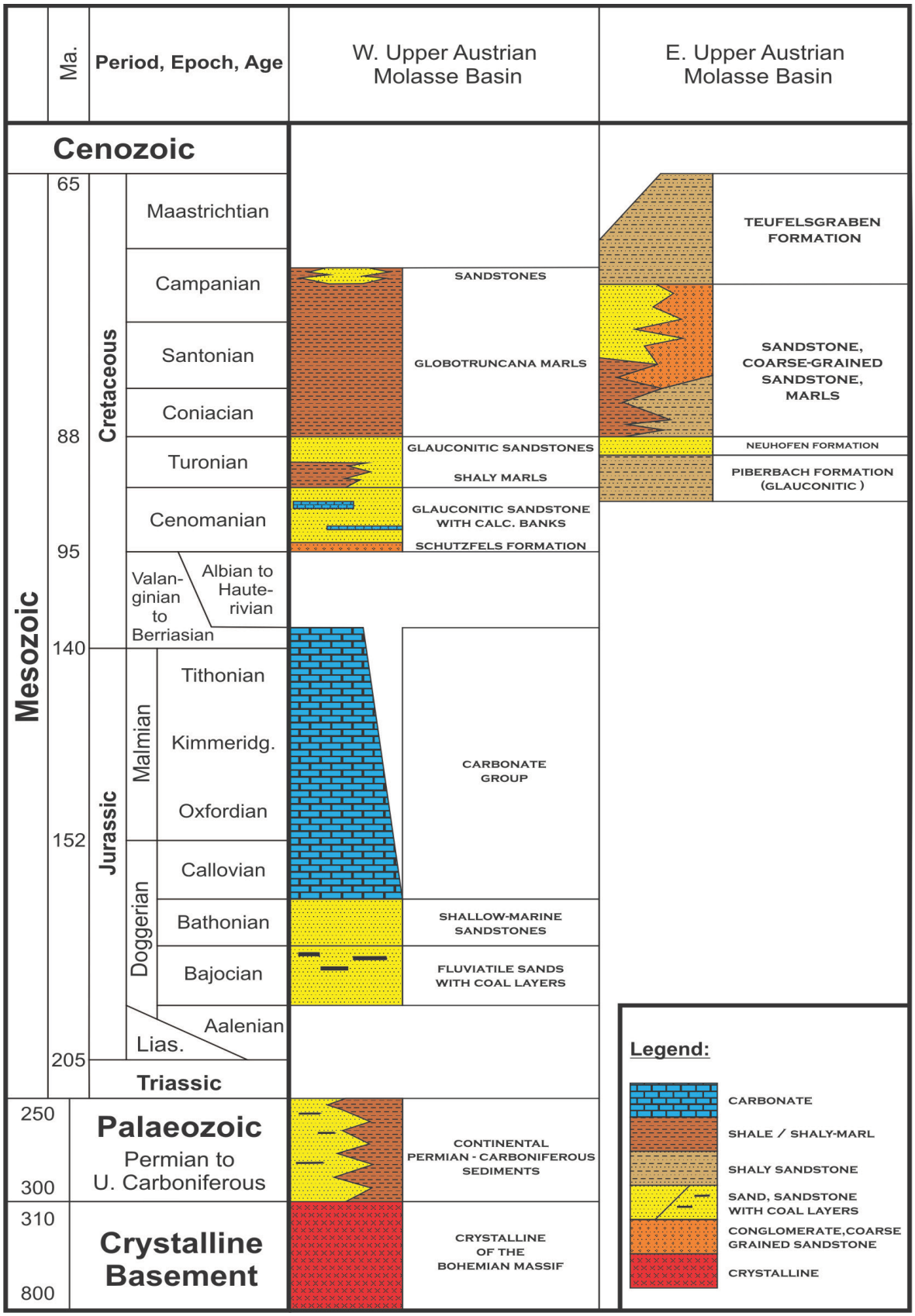

Fig. 5: Stratigraphic chart of Palaeozoic and Mesozoic in the Upper Austrian Molasse Basin, modified from Malzer et al. (1993)

During early Cretaceous times the carbonate platform of southern Germany was tectonically uplifted, together with the Jurassic carbonates in the Upper Austrian Molasse Basin. Locally the Jurassic sediments were heavily eroded and karstified. With the exception of greenish glauconitic sandstones and dark marine marls south of the Central Swell, no lower Cretaceous sedimentary record is preserved in the Molasse Basin (Malzer, et al., 1993).

The oldest preserved Cretaceous sediments are the coarse grained fluviatile sands of the Schutzfels Formation (Cenomanian), which infill Jurassic karst structures down to a depth of 100 m below the Jurassic surface. After deposition of the Schutzfels Formation a major marine transgression from SW took place, which led to the deposition of storm influenced sediments. Those glauconitic sandstones were deposited on the broad shelf below the storm-wave base and reach a thickness up to 70 m. They are characterised by a rhythmical succession of thinly laminated storm layers with hummocky cross bedding and escape burrows of organisms. The on-going subsidence of the area is reflected by sedimentation of shaly deep-water marls during early Turonian times. Underlain by a bed of glauconitic sandstone that was transferred to outer shelf regions by storm energy, the deposition of Globotruncana bearing shales and marls continued south of the Central Swell up to late Campanian. Northwest of the Central Swell 300 m thick strata of shallow water sandstone have been deposited, that reach past the Central Swell to the south where they interfinger with the shales and marls. The maximum thickness of Cretaceous sediments encountered in wells is about 800 m. (Malzer, et al., 1993; Wagner, 1998).

In the eastern part of the Upper Austria Molasse Basin, the upper Cretaceous deposits show at the base the same trend as in the western part. The Turonian glauconitic Piberbach Formation corresponds to marine storm impacted sediments. Above the Piberbach Formation, the evolution is different compared to the western part of the basin. An increase in terrestrial influence is recorded by the deposition of the deltaic sandstones of the Neuhofen Formation. Terrestrially influenced Sediments (sandstone) with interbedded marls overlie the Neuhofen Formation. The youngest Cretaceous sediments are represented by the Teufelsgraben Formation, composed of limnic-terrestrial shales, in the eastern part of the Basin. In total, these sediments reach a thickness of approximately 700 m in the eastern part of the Upper Austrian Molasse Basin

and terminate at the Steyr fault in the east (Malzer, et al., 1993). The distribution of Mesozoic sediments is shown in the Pre-Tertiary subcrop map in Fig. 6.

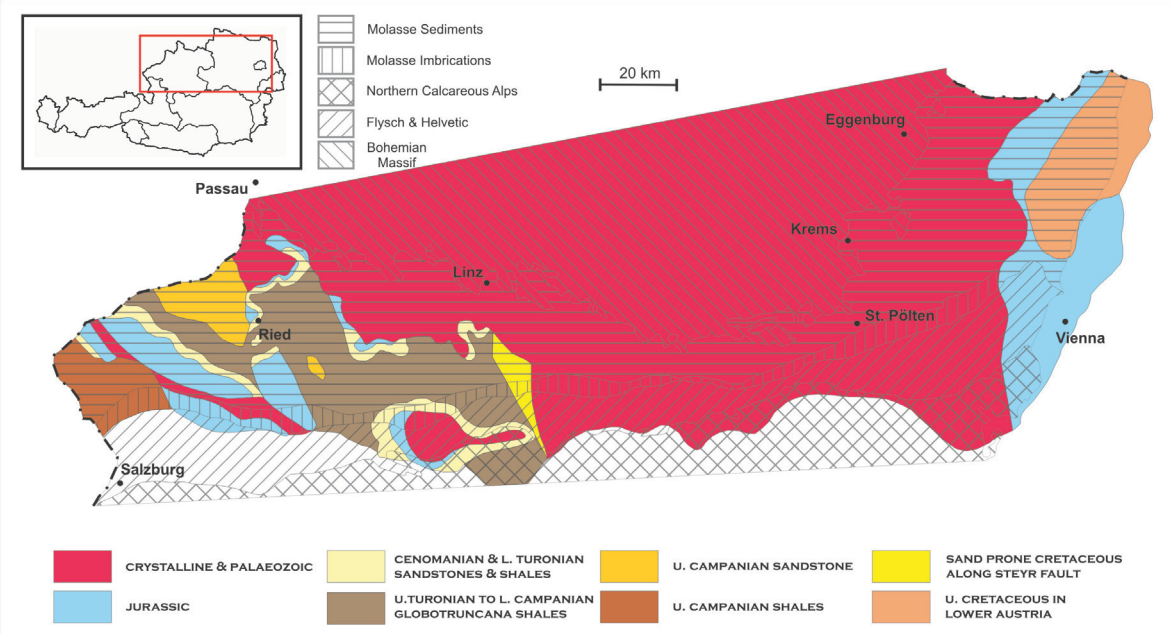

Fig. 6: Pre-Tertiary subcrop map of the Austrian Molasse Basin. The present day tectonic situation is shown as an overlay; modified from Wagner (1998)

At the end of Cretaceous times the European plate was uplifted, due to the beginning collision with the African-Adriatic plate after complete subduction of the Penninic Ocean. The combination of uplifting and eustatic sea level low stand caused the subaerial exposure of the area of the Austrian Molasse Basin and led into a phase of intense erosion, during which Mesozoic sediments up to 1600 m thick were eroded. As a result, a smooth, southward dipping plane developed that was dissected into several blocks by reactivation of existing fault systems. This setting remained unchanged until Eocene times (Bachmann, et al., 1986; Malzer, et al., 1993).

Cenozoic Setting

In the late Eocene the Thetys Sea transgressed across the segmented plane of crystalline basement and its Autochthonous Mesozoic cover. The Central Swell, as morphologic high zone, acted as barrier between the lagoon and the open marine realm. Therefore the beds of this time characterise the transgressive setting (Fig. 7). North of the Central Swell the limnic series of the Voitsdorf Formation consisting of red, green, yellow and white clays, cut by channels of meandering rivers was deposited. It is locally capped by approximately 4 m of swamp coal that is overlain by the soft shales of the paralic Cerithian Beds, which are cut by tidal channels as well. Finally shallow marine sands indicate the transition to fully marine conditions (Wagner, 1998).

On the Central Swell the red algae and coral reefs of the Lithotamnium Limestone developed that shed their debris to the northern lagoon as well as to the southern high energy shelf environment. At least three cycles of subsidence and shallowing can be identified within these beds. The reef body itself is preserved as dense light grey to yellowish limestone, while the shed debris formed grey to brown limestones that extend over large areas of the basin. To the south in direction of the open sea they interfinger with the Nummulitic Sandstone that was deposited at a water depth of approximately 50 m. At a depth > 80 m greenish – grey shales and marls of the Perwang Formation (Discocyclina Marl) replace the Nummulitic Sandstone. Globigerina Limestone and marl of the Nussdorf Formation follow southward at greater water depths (200 m). The occurrence of the light grey to brown Miliolid Limestone is restricted to the tectonic slices of the imbricated Molasse and pebbles in Oligocene turbidites (Malzer, et al., 1993; Sissingh, 1997; Wagner, 1998).

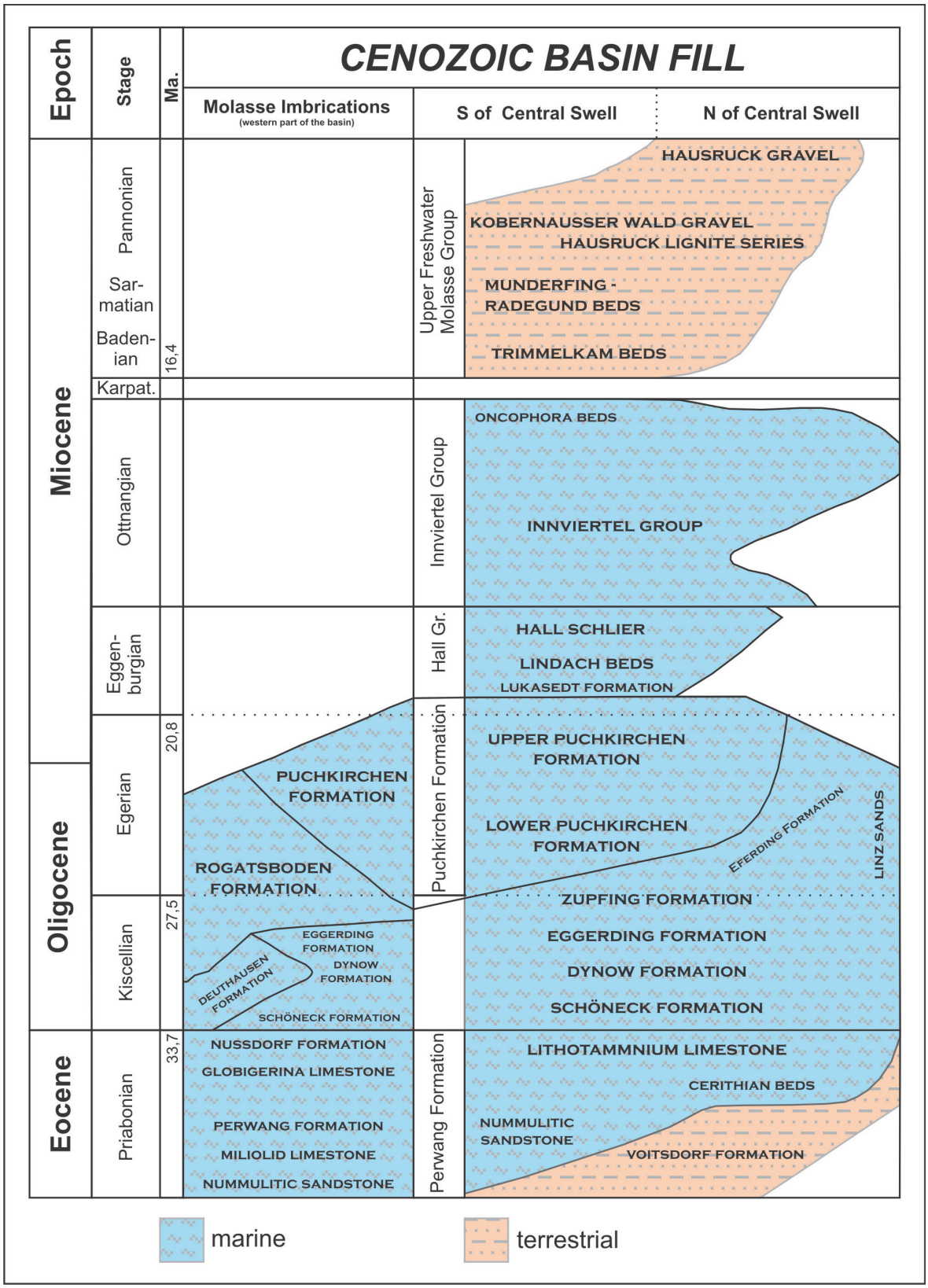

Fig. 7: Stratigraphic chart of the Cenozoic basin fill, modified from Wagner (1998)

During Oligocene times, dense and cool bottom sea currents were forced to deviate from their former flowpath, because of the tectonically northward moving slope. As a result of the dislocation, the southern slope as well as the slope to the north (in a minor extend) were undercut by the erosional impact of these currents which lead to over - steepening of the flanks. Massflows occurred from the north and the south that are preserved in calcitic turbidites of the Deuthausen Formation and the distal turbidites and contourites of the Rogatsboden Formation. Both formations can be found in Austria only in the Molasse Imbricates but crop out in Bavaria, where complete Bouma sequences were identified within the Deuthausen Formation (Wagner, 1998).

The on-going deepening and widening of the area of sedimentation resulted in the drowning of the Eocene carbonate platform and the cool and dense deep-water flows were overlain by shallower, warmer Thetyan currents of higher salinity. The difference in temperature enhanced the formation of a halocline that was accompanied by oxygen depletion of deeper water levels (dysoxic to anoxic conditions). In this environment the most important source rock of the Molasse Basin was deposited: the Schöneck Formation (also referred to as Schöneck Fishshale). It is composed of dark grey to black shales and marls. The Schöneck Formation reaches a thickness up to 30 m and interfingers to the north with a small belt of shore sands. In middle Kiscellian times, the salinity of shallower water layers decreased as a result of increased fresh water influx. This resulted in a break-down of the water stratification and an increase of oxygen content in deeper water levels (Malzer, et al., 1993; Sissingh, 1997; Schulz, et al., 2002).

This situation marks the transition from the Schöneck Formation to the overlying Coccolithian marlstones of the Dynow Formation that has a relatively low TOC content. The appearance of Coccoliths is an indication for deep water conditions. In detail this means a depth of deposition of several hundred meters water depth and a low energy environment. An increase in terrigenous influence is notable in the sediments of the Eggerding Formation on top of the deep marine deposits of the Dynow Formation. It consists of 35 to 45 m thick alternating layers of grey laminated pelites and Coccolithian marl in the lower part and homogenous marly shale in the upper part. The Eggerding Formation was deposited in an oxygen deficient environment at the northern slope of the Molasse Basin, resulting in TOC contents of 1.6 % – 5 % and was locally removed by submarine mass movements (Sachsenhofer, et al., 2010). The Eggerding Formation is

overlain by the Zupfing Formation, an up to 450 m thick succession of brown clay marl and dark limestone. Oxygen deficient conditions continued during deposition of the lowermost few meters ("Transition Zone"), causing TOC contents of 1.5 %. The Zupfing Formation is interpreted as the distal parts of turbidites from the south, but it also contains slumps and slides from the north, accumulating predominantly at faults (Wagner, 1998; Sachsenhofer, et al., 2010).

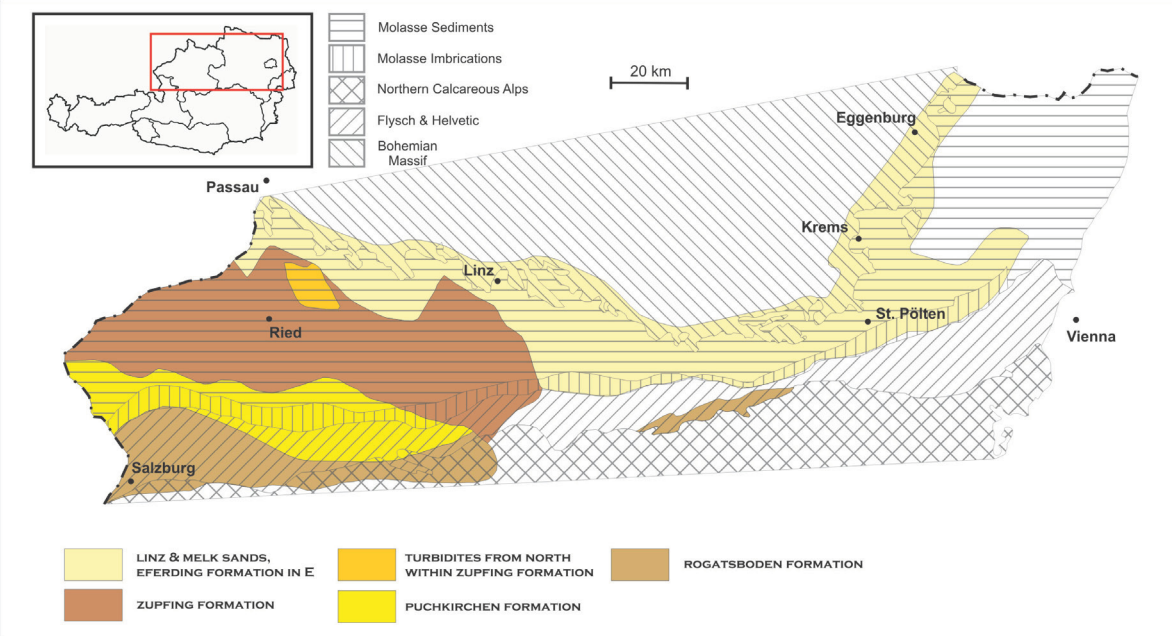

Fig. 8: Mid-Oligocene facies distribution in the Austrian Molasse Basin (subcrop map). The present day tectonic situation is shown as an overlay; modified from Wagner (1998)

While sedimentation of the Molasse Basin was dominated by input from the northern or southern flank, in early Oligocene to Miocene times the E-W trending (along the axis of the basin) low sinuosity channel belt of the Puchkirchen Formation developed. It was 3 – 6 km wide and more than 100 km long (Fig. 9). Within this setting, a wide variety of sediments have been deposited, including conglomerates, sandstone, silt- and mudstone in a water depth of approximately 1000 – 1500 m. Apart from the axial channel belt, two other depositional elements of the Puchkirchen system could be identified in 3D seismic data: Slope fans on the southern flank of the Molasse Basin and Puchkirchen sediments resting transgressively on top of the Molasse Imbrications – the fill of piggyback basins. The Puchkirchen Formation reaches a thickness of up to 1500 m, although erosion occurred in the upper Puchkirchen Formation (De Ruig, et al., 2006; Covault, et al., 2009; Hubbard, et al., 2009).

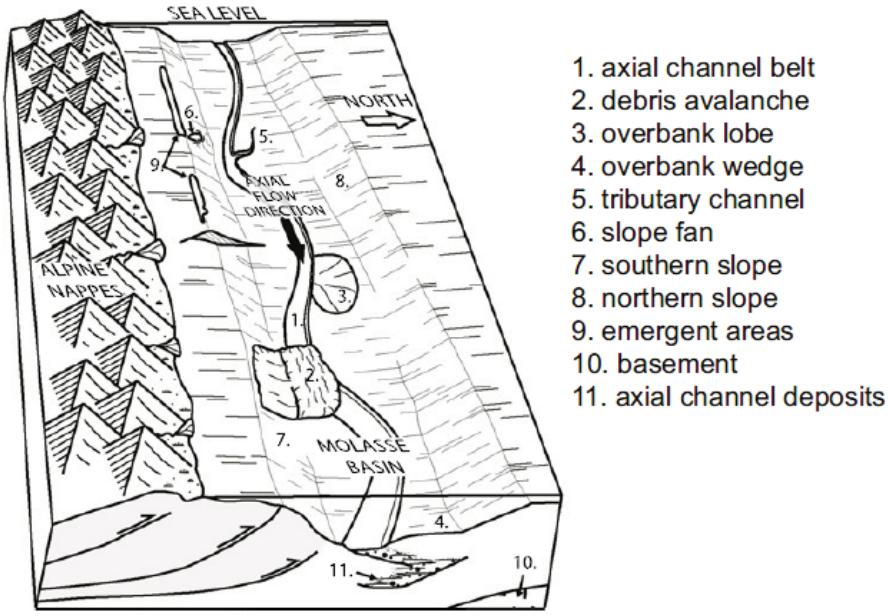

Fig. 9: Schematic reconstruction of the Molasse Basin during deposition of the Upper Puchkirchen Formation showing the distribution of depositional elements (Hubbard, et al., 2009).

To the north, the Sediments of the Puchkirchen Formation interfinger with the Egerian shore facies, preserved as Linz/Melk Sands. The material was shed from the Bohemian Massif, due to the high feldspar content that indicates a short distance transport (Malzer, et al., 1993).

In Oligocene the consequences of the flexure of the European Plate become obvious. E – W trending extensional faults develop in that dissect the basement into blocks and elements of the basin were influenced by or incorporated in the Alpine thrust sheets. This situation continues up to lower Miocene, where the Molasse Imbrications reach approximately their present day position. From this time on the uplift of the Alps is the dominant process in basin evolution (Malzer, et al., 1993; Wagner, 1998).

During lower Miocene, after the most prominent submarine erosion in the Molasse Basin that marks the base of the Hall Group, the Lukasedt Formation was deposited in a relative narrow erosional channel on top of the Molasse Imbrications. The channel was filled by slides and slumps, turbidites and contourites at a water depth of approximately 500 m and uplifted with the imbrications. Today, these sediments crop out at an elevation of 500m north of Salzburg. This corresponds to an uplift of 1000m in the last 20 Ma. With the northward moving imbricates, the zone of submarine erosion was shifted to the north and the same scenario of sedimentation took place in a newly formed channel – the

Lindach Formation was deposited. The basinwide dominant sediment of this time is the so called Hall Schlier. It consists of light grey sandy pelites that are interpreted as distal parts of turbidites and contourites. In the lows of the basin, the turbiditic and contouritic sandstones accumulated. Including the Lukasedt Formation, the sediments of the Hall Group can reach a thickness of 800 m (Malzer, et al., 1993; Wagner, 1998).

The Ottnangien is characterised by a transgressional setting with on-going shallowing of the Molasse Sea. This evolution is preserved within the sediments of the Innviertel Group that is built of alternating shale prone and sand prone beds. Sedimentary structures like tidal induced crossbedding and ripplemarks are very common, as well as burrows of organisms. At the peak of the transgression the sea reaches past the Bohemian Massif to the north, before from Bavaria to the east shallowing set in and fresh water influx lead to a decrease in salinity. In this environment the Oncophora beds were deposited, consisting of well laminated, mica bearing fine sandstones with interbedded mudstones. At the beginning of Karpartien, the sea regressed from the Alpine foreland and the Ottnangien sediments were partly eroded (Malzer, et al., 1993; Wagner, 1998).

After the period of subaerial erosion throughout the Karpartien, terrigenous sedimentation set in at Badenian times: the Upper Freshwater Molasse Group. At the base of the succession, the Trimmelkam Beds can be found that consist of limnic pelites and the sandstones of meandering rivers. In the area of the river Salzach and further to the east coal seems developed. Above the Trimmelkamm Beds, the braided river sediments, pelites and lignites of the Munderfing-Radegund Beds were deposited. During Pannonien the Hausruck Lignite Series developed and was capped by the fluvial gravel of the Kobernauser Wald and the Hausruck (Malzer, et al., 1993; Wagner, 1998).

From Pliocene on a period of erosion set in in the whole Molasse Basin. No sediments were preserved from that time. In Pleistocene wide parts of the Molasse Basin were covered with gravels and moraines that can reach a thickness of 30 m (Malzer, et al., 1993).

The Allochthonous and Parautochthonous Molasse Evolution

Besides the Autochthonous Molasse and the Imbrications (Allochthonous Molasse), sediments resting unconformably on top of Alpine tectonic units or Molasse Imbrications are present near the Alpine thrust front in the south of the basin. These are referred to as the Parautochthonous Molasse (Steininger, et al., 1986).

In many thrust belts the limit of significant topography is far to the rear of the frontal thrust that is often covered by large amounts of synorogenic sediment. The sediment that accumulates on top of the frontal thrust sheets constitutes the wedge top depozone, including piggyback, thrustsheet-top or satellite basins. The sediment deposited in those areas is typically composed of subaqueous mass flows and fine grained shelf sediments that are texturally and compositionally immature. Wedge top depozones taper onto the orogenic wedge and are characterised by several features such as the abundance of unconformities and various types of growth structures, indicating that erosion and syntectonic deformation are important aspects in the formation of those sediments (DeCelles, et al., 1996).

In the Molasse Basin the frontal thrust system, on which the sediments of the Parautochthonous Molasse were deposited, is formed by the Molasse Imbrications that were overthrusted in Miocene times by the overthrust system (Fig. 10).

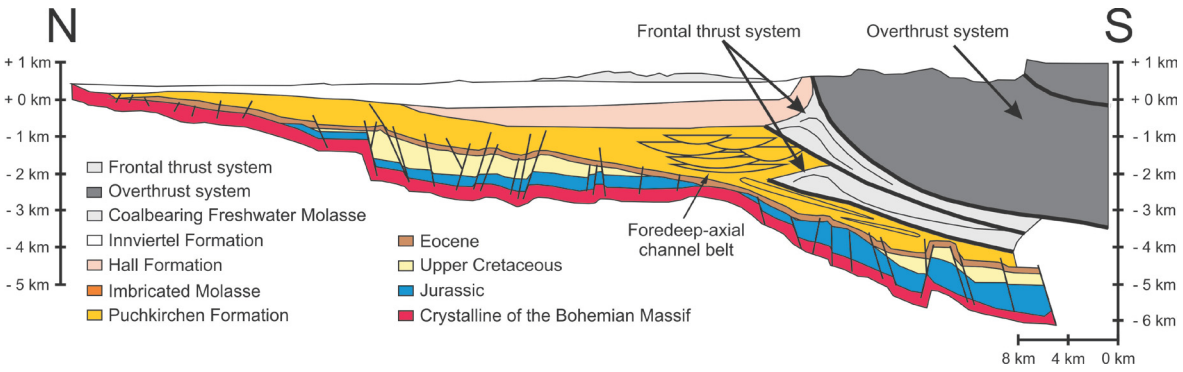

Fig. 10: N – S cross section through the Molasse Basin demonstrating Positions of frontal thrust and overthrust system, modified from Wagner (1996) and De Ruig (2006)

The NNW-verging frontal thrust system is composed of a forward propagating series of at least five thrust faults. The hindward-most thrust sheet is composed of middle Egerian lower Puchkirchen sediments at its stratigraphic highest position; therefore the onset of thrusting has occurred following middle Egerian deposition of the lower Puchkirchen sediments. Late Egerian upper Puchkirchen sediments lap onto the forward most

thrustsheet, suggesting that thrust movement stopped before that time (Fig. 11). The frontal thrust system is structurally overlain and truncated by the overthrust system, therefore thrust movement in this system has to be younger than in the frontal thrust system (Covault, et al., 2009).

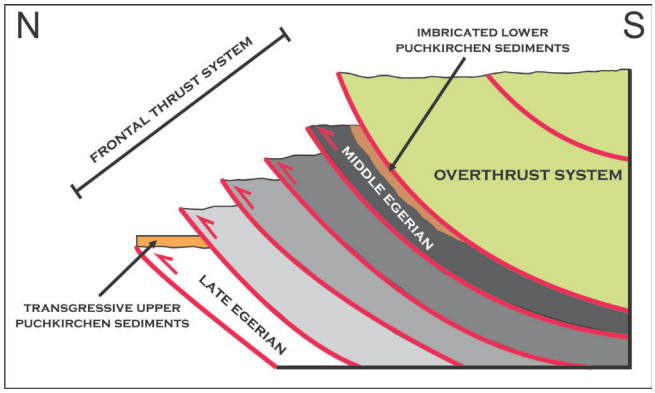

Fig. 11: Sketch illustrating thrust movement and age relations in the Molasse Basin

The frontal thrust system is segmented by en-echelon oblique to the thrust orientated structures that allow strike-slip movement and lengthening of the system in an E-W direction. Those structures do not extend into the foredeep and their hindward extend is undetermined due to poor seismic quality. They seem to provide a mechanism for transferring displacement between pairs of existing thrust faults and are interpreted as secondary tear faults, which facilitated the evolution of canyon-channel systems across the foredeep-margin slope (Covault, et al., 2009).

Piggyback Basins

Piggyback basins are basins that formed and are carried on active thrust sheets (Ori, et al., 1984). At least two of those basins (Lauterbach Basin, Nussdorf Basin) are known in the Austrian Molasse area on top of the frontal thrust system. They are crescent to circular shaped in plan view, and ponded to wedge shaped in profile. Basin floors developed relatively flat, while basin margins locally approach gradients as great as 40° as a result of deformation synchronous with and following sedimentation in the basin. This circumstance can be explained by the presence of growth strata. This suggests that those basins formed by a process named piggyback-thrust propagation, in which the frontal ramp of a thrust sheet becomes inactive and a new ramp forms in front of the old one. The internal stratigraphy of piggyback basins is also controlled by the local thrust movement, resulting in complex angular unconformities as a result of modification of the topography during sedimentation (Butler, 1982; Zoetemeijer, et al., 1993; Covault, et al., 2009).

Depositional Environment and Lithofacies Associations

Within the wedge-top depozone, gravity induced mass flows are the most prominent elements in deposition and erosion (sediment bypassing). The slope fans and piggyback basins of the Austrian Molasse Basin are filled by complex turbidite systems with a north oriented direction of transportation (from the overthrust system to the basin). Following Covault (2009), several facies associations can be distinguished in this setting:

Facies Association 1 (FA1): upward fining and thinning turbidites

FA1 describes an up to 35 m thick unit of massive to normally graded sandstone overlain by interbedded mud-/siltstone and sandstone intervals. Locally those beds exhibit disturbed fine grained units on top, interpreted as remains from slumps and slides. FA1 shows a fining upward trend and also thinning of sections to the top, while the massive sandstone composes more than the half of the unit. Stacked series of those beds can reach a thickness of 100 m.

The massive sandstone section is interpreted as the remains of high fallout rates from coarse grained high density turbidity currents. The overlying beds represent sediment deposited by fine grained turbidity currents after settling of the high density load. The fining and thinning upward within the unit may reflect proximal – distal stacking of those events. FA1 represents the consequences of periods of tectonically induced sediment failure followed by quiescence along the frontal thrust system. The turbidites may have transformed from slumps and slides or debris flows when the flow becomes longitudinally segregated. Coarse grained sediments concentrate at the top of the flow, finer grained sandy sediment at the back. When the flow loses its competency to carry sediment, the back part of the flow outruns the front and turbulence and water entrainment leads to flow transformation to turbidity currents that might deposit long distances from the original sediment failure.

Another possible explanation for the evolution of FA1 is the deposition by canyon-channel system migration. However, 3D seismic data does not show any canyon or channel features within the wedge top depozone, which also might be caused by the fact that those features are present at a scale smaller than seismic resolution (Covault, et al., 2009).

Facies Association 2 (FA2): amalgamated thick-bedded turbidites and debris flow deposits

FA2 deposits are composed of up to 50 m thick beds of amalgamated, thick bedded, predominantly structureless coarse grained sandstones and local sand rich, muddy matrix conglomerate. Sandstone beds are universally micaceous and rich in fossiliferous detritus. They also contain large, extrabasinal igneous, metamorphic or carbonatic clasts (> 30 cm in diameter). Stacked successions of those units can reach a thickness of 180 m.

The deposition of FA2 is related to high density turbidity currents. The beds are structureless and contain large extrabasinal clasts, which indicate a more proximal position of deposition compared to FA1. The finer sections present in FA1 might have been eroded. Another possibility would be that the sediments of FA2 might reflect a steady depletive flow that requires constant discharge sustained for long periods of time, such as might be generated by fluvial input. The mud-matrix conglomerates within the succession are the results of en-masse freezing of cohesive debris flows. This can be reached when the driving gravitational force decreases below the strength of the flow (Covault, et al., 2009).

Facies Association 3 (FA3): chaotic mass

The beds of FA3 consist of up to 30 m thick disorganized lithofacies, like disturbed thin bedded mud-/siltstone and sandstone or mud-/silt matrix conglomerate. Water escape structures in the sandstones and intraformational clasts are common features.

These deposits are the result of sediment failure and slumping/sliding. The intraformational clasts indicate a local sediment source and a wide ranging grain size distribution suggests a short distance of transportation and no transformation to debris flows or turbidity currents (no sorting due to gravitational flows). Immediately after the sediment failure, the flow accelerates down the steep slope (e.g. piggyback basin margin) followed by a rapid deceleration and deposition at the break of the slope (e.g. piggyback basin floor). Like in FA1 the initiation of sediment failure is the tectonic movement of the frontal thrust system (Covault, et al., 2009).

Petroleum System

Within the Molasse Basin, two separate working petroleum systems can be found: One involving thermogenic hydrocarbons and one with hydrocarbons of biogenic origin.

The source rocks for the thermogenic hydrocarbons are formed by the Schöneck Formation and the upper intervals of the Eggerding Formation, both with TOC contents of approximately 1,5 – 5,5 % and mean HI values of 500 – 600 mgHC/gTOC (Schulz, et al., 2002; Sachsenhofer, et al., 2010). The sediments are immature at shallower parts of the basin, but due to their wide lateral extend their presence underneath the Alpine nappes can be expected and in that position their maturity is granted as a result of higher burial depth and therefore higher temperature. The fact that the source rocks are immature in shallower areas of the basin, where almost all reservoirs of thermogenic hydrocarbons are situated, suggests long distance lateral migration (> 75 km) from the source kitchen underneath the Alps to the reservoirs. This is supported by the fact, that the source rocks are found in a stratigraphically higher position than the reservoir rocks. Therefore migration across faults during upper Oligocene (Fig. 12), with juxtaposition of older reservoir rocks against younger source rocks is a likely model for migration in the Austrian Molasse Basin (Malzer, et al., 1993).

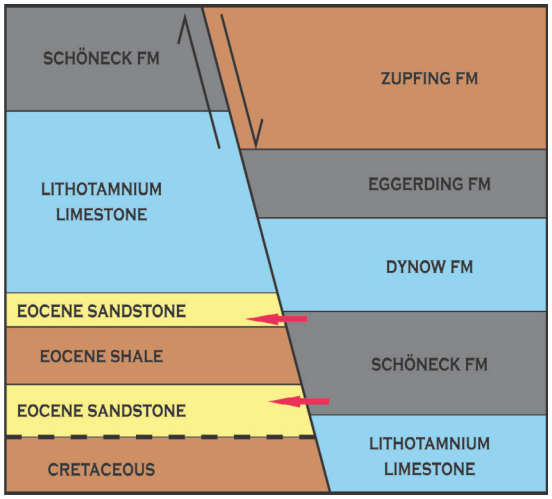

Fig. 12 : Schematic illustration of migration across faults in the Molasse Basin, modified from Malzer et al. (1993)

Reservoir rocks as well as seals can be found in various positions in the stratigraphic succession (Fig. 13), but the most important reservoirs for thermogenic hydrocarbons are the Eocene sandstones. Almost all thermogenic hydrocarbon bearing reservoirs formed at structural traps, where north-verging faults juxtapose tight marls and shales of the Zupfing Formation against Eocene reservoir rocks.

No thermogenic hydrocarbons occur within the reservoirs of the Puchkirchen and Hall Formation, because of the fact that there is no fault related connection to Eocene. The gas in those reservoirs is of bacterial origin (98% methane) and was generated shortly after deposition. Stratigraphic traps within the formations form the barrier for hydrocarbon migration (Malzer, et al., 1993).

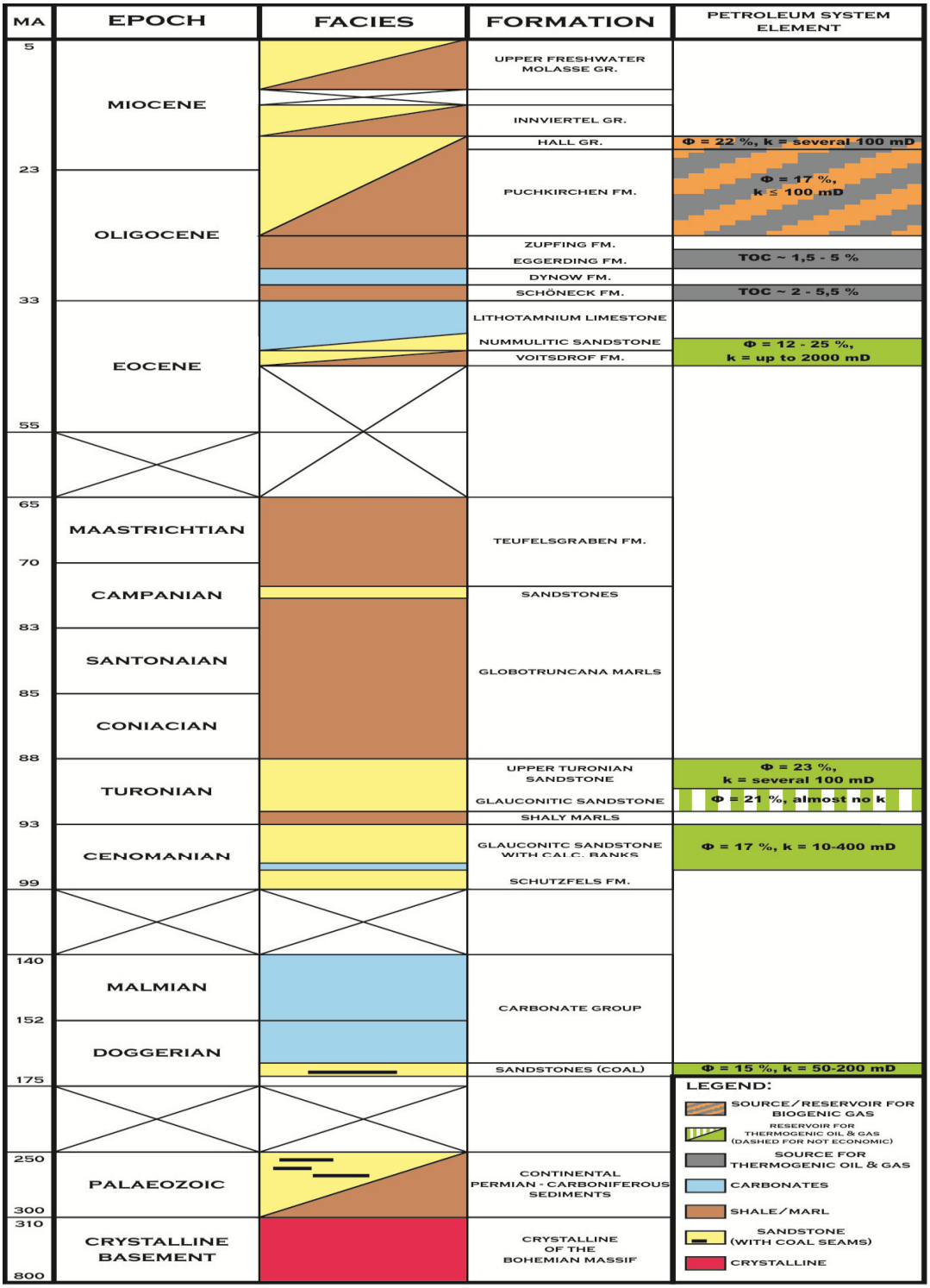

Fig. 13: Stratigraphic chart of the Upper Austrian Molasse Basin illustrating elements of the petroleum system, based on data from Malzer, et al. (1993)

The Lauterbach Basin

The Lauterbach Basin is located at the border of Salzburg and Upper Austria above the Molasse Imbrications near the thrust front of the Alps (Fig. 14).

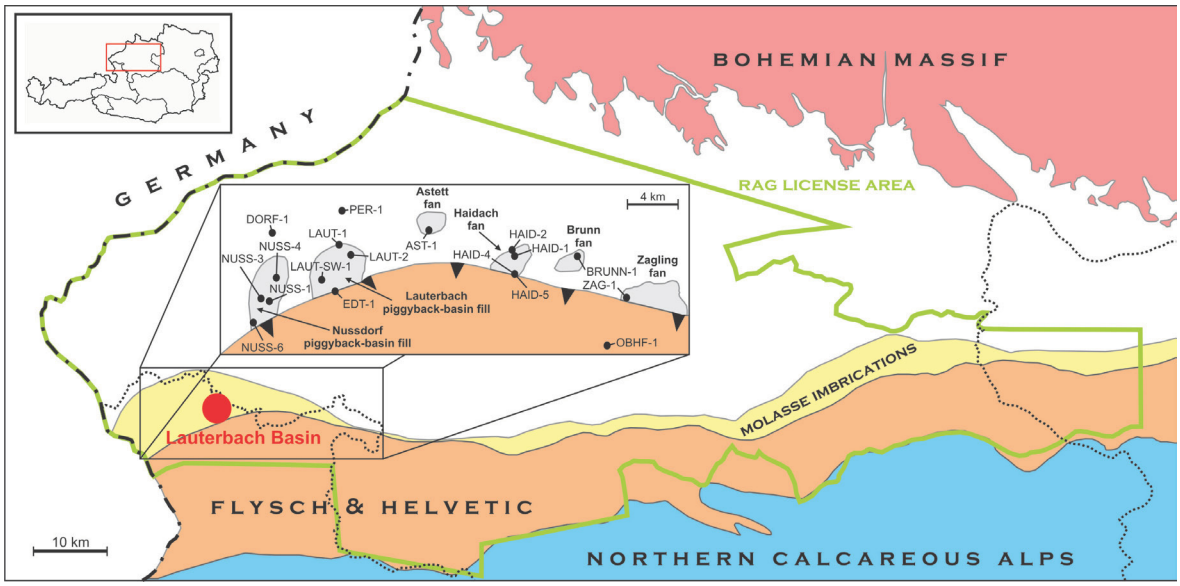

Fig. 14: Location of the Lauterbach Basin, map modified from RAG and Covault et al. (2009)

It is a piggyback basin that developed on top of the thrust sheets of the frontal thrust system. It is approximately < 5,5 km long and < 3,5 km wide. The original extent of the basin is difficult to determine, due to truncation by the overthrust system in the south. The thickness of the basin fill can reach up to 450 m and consists of turbiditic sediments of the Upper Puchkirchen Formation, deposited during late Oligocene and early Miocene times.

The rather steeply dipping basin margins (locally 40°) form a zone of flow convergence (acceleration and accumulative behaviour), whereas the flat basin floor forms a zone of flow divergence (deceleration and depletion). At the base of the basin margin fine grained sediments of FA3 can be found, while the rest of the basin fill consists predominantly of FA1 units that contain reservoir quality sandstone layers (Covault, et al., 2009).

Geological Conception of the Lauterbach Gas Field and its change through time

The exploration activity in the Lauterbach Basin started with the well Laut-001 in 1995. The purpose of the well was to investigate a potential gas bearing structure in the Upper Puchkirchen Formation 2 km to the west of the well Bern-001 (Fig. 15). The well encountered three zones with reservoir potential (from deep to shallow): the water bearing A2L50 interval and the layers A2L40 and A2L30 with a net thickness of 6.4 m, both gas bearing. With the well Laut-002 both gas bearing horizons should have been developed in a structural higher position, but were encountered in a low permeable facies condition. The A2L50 zone however was hit in a 45 m structural higher position with good reservoir properties and gas charge. Therefore the well Laut-003 was drilled to develop the layer A2L50 in an even better position, but only the upper part (3.7 m net thickness) was met with sufficient porosity. The purpose of the well Laut-004, drilled in 2006, was to hit the interval A2L30 in a better facies condition in the north of the well Laut-001, unfortunately with little success.

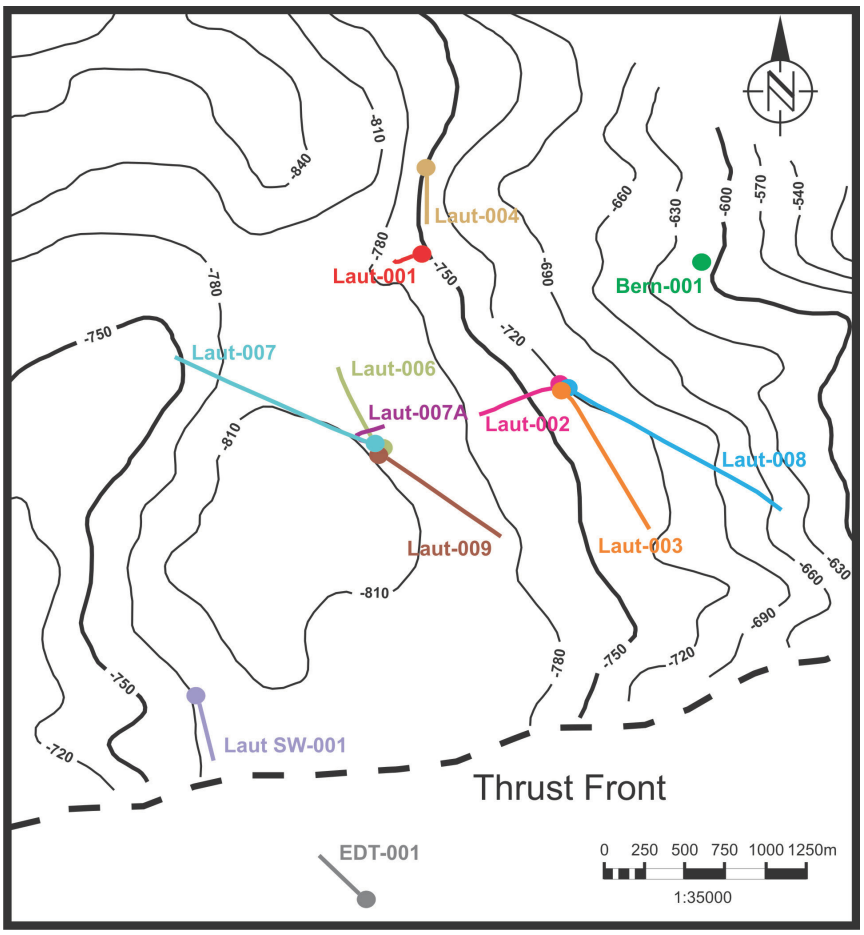

Fig. 15: Location of wells in and near the Lauterbach Basin, underlain by a structural map of the base of the Lauterbach Basin in TWT [ms] to highlight structural high and low positions

In the meantime, the well Laut-001 produced almost 10 years with very little pressure decline. This led to the understanding that reserves were underestimated in the first place and that the reservoir has a wider extent than expected (Fig. 16).

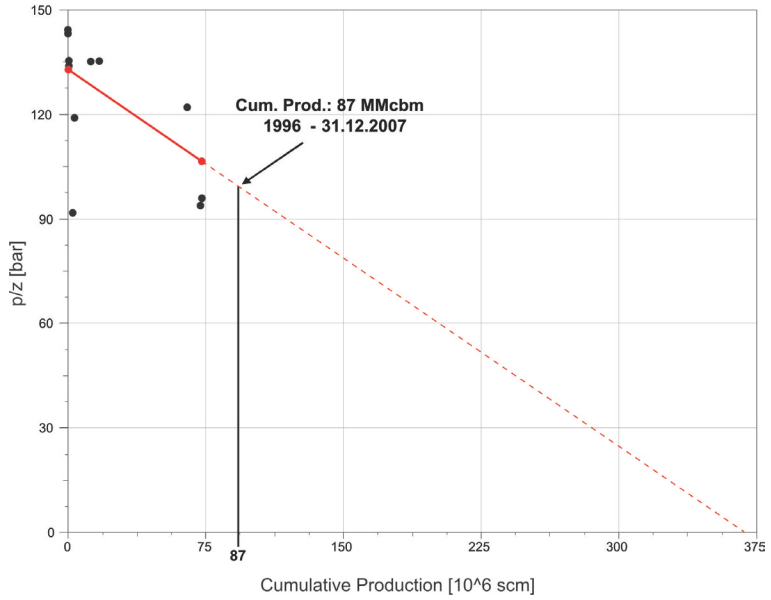

Fig. 16: p/z - plot of the well Laut-001 indicating large reserves

With all four wells situated at the eastern flank of the Lauterbach Basin (structural high), Laut-006 was the first well to be drilled in the centre of the basin – with great success: The layers A2L40 and A2L30 were encountered with good reservoir properties and gas bearing in greater gross and net thickness above the uniform gas-water-contact (GWC) of the Lauterbach gas field (-810 m NN). Due to the fact that the pressure of both layers was below initial pressure, the assumption of the existence of a communication between the intervals of Laut-001 at the basin flank and Laut-006 in the centre of the basin was validated. Additionally another reservoir horizon above A2L30 was hit at initial pressure, referred to as A2L27/1. With the well Laut-007 the western part of the basin should be investigated and the A2L40 and A2L30 intervals developed to produce outside the drainage area of Laut-006. Unfortunately A2L30 pinches out and is therefore not present in the western part of the basin, while A2L40 was hit below the GWC. Laut-007 was side-tracked to the northwest and encountered A2L40 and A2L30 gas bearing and in similar condition as in Laut-006.

The well Laut-008 should encounter A2L50 in its structural highest position on the eastern basin flank. This was achieved, but reservoir conditions were not sufficient in this interval. The last well drilled in the basin, Laut-009 in 2010, had the purpose to develop A2L40 and A2L30 in the southern part of the basin. Several productive horizons were encountered:

- A2L27/2: new interval at initial pressure
- A2L27/1: already hit in Laut-006
- A2L30
- A2L50: below GWC

One of the main targets, A2L40, pinches out before the subsurface location of Laut-009. There is already a next well planned, Laut-010, which will be drilled into the southern part of the basin. It will surely deliver new insights into this complex reservoir in the wedge top depozone.

Data, Methods & Workflow

This study was carried out using a 3D - seismic dataset and data from 12 wells within or in the vicinity of the Lauterbach Basin provided by RAG.

The seismic data (Lamprechtshausen 3D) was acquired in 1993 covering an area of 145km^2 (Fig. 17), using a vibroseis source with a sweep of 14 – 90 MHz and a sampling rate of 2 ms. For the purpose of easier data handling a cropped volume of the Lamprechtshausen 3D cube was used for the evaluation of the Lauterbach Basin.

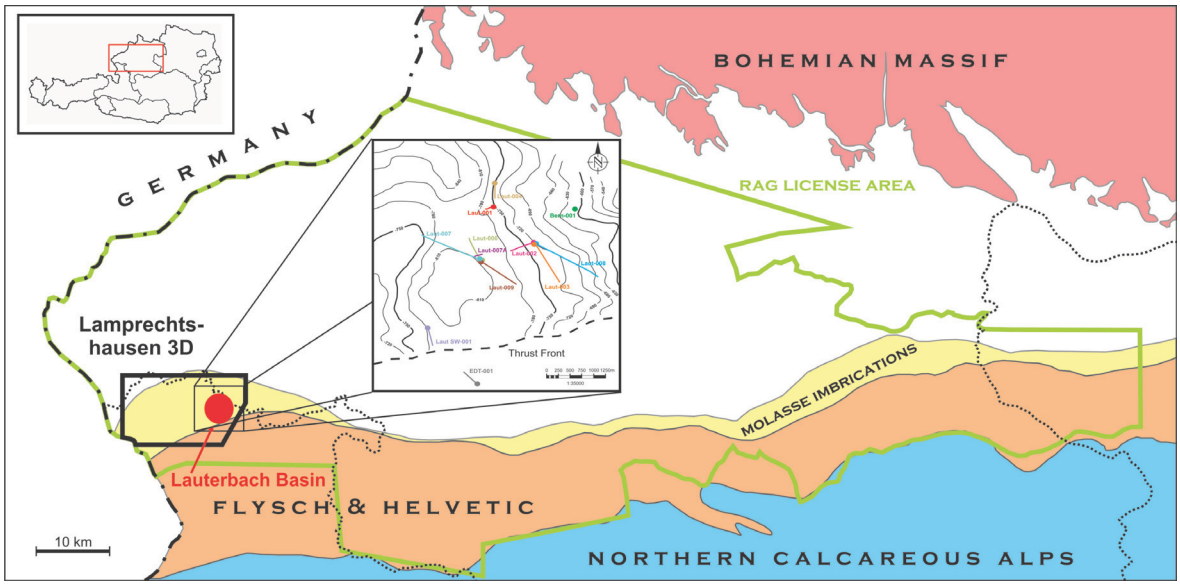

Fig. 17: Location of seismic cube "Lamprechtshausen 3D" and wells in the Lauterbach Basin

12 Wells are located in the study area, ranging in age from 1995 (Laut-001) to 2010 (Laut-009). From every well, the following suite of well logs is available:

- Sonic Log
- Gamma Log
- Resistivity Logs (deep, shallow, micro)
- Density Log
- Neutron Log
- SP Log

Core data from selected intervals is provided for the wells Laut-006 and Laut-007.

Log correlation was carried out using sonic, gamma and resistivity logs as well as pressure data from the different productive horizons. Sand bodies in stacked turbidite systems often show similar log-patterns, therefore pressure data provide additional help in identifying the same layers in different wells.
Seismic interpretation can be rather challenging as well. Changing facies and erosional events below seismic resolution lead to different geologic conditions along a single apperantly continuous reflector. Amplitude variations can be an indication for varying bed thickness (Chadwick, et al., 2004).

In the geological model seismic data was used as input for defining the geometry of the productive zones. Due to the fact that top and base are not separately mappable, because of a layer thickness smaller than seismic resolution, the mapped reflectors were chosen to define the geometry of the top of each sand body. The base of each horizon was defined by constructing thickness maps, generated from well data and amplitude trends. The volume of each layer was defined by adding the thickness of the zone to the mapped horizon top. For the purpose of a dynamic simulation, the intervals between the sand bodies were defined as barrier layers that provide an on/off – switchable path of communication between the productive zones.

The internal structure of the sand bodies was modelled by introducing facies zones that reflect the three prominent facies conditions in the reservoir, derived from the gamma log. The cells of the model were filled with those three facies zones not only in a stochastic way but also with a special focus on geobodies that form in a wedge-top environment (“object based modelling”).

Results

Well-log Correlation

The well-log correlation is the important first step in building a geological model of a reservoir. It allows the definition of exact well tops for a later seismic interpretation and the estimation of lateral extent and thickness of intervals of interest. Thicknesses derived from the well-log correlation form also a main input for thickness maps needed in the geometric modelling process.

In the Lauterbach Basin, the well LAUT-006 was chosen as reference well to define the zones of interest (Fig. 18). Due to its position in the centre of the basin, it encountered most of the productive layers in high thickness and therefore in best condition for characterisation. Starting from this well, two sections were correlated (Fig. 18). Well section 1 is trending approximately N-S (Laut-001 – Laut-006 – Laut-007A – Laut-009) and well section 2 W-E (Laut-007 – Laut-006 – Laut-002 – Laut-003 – Laut-008).

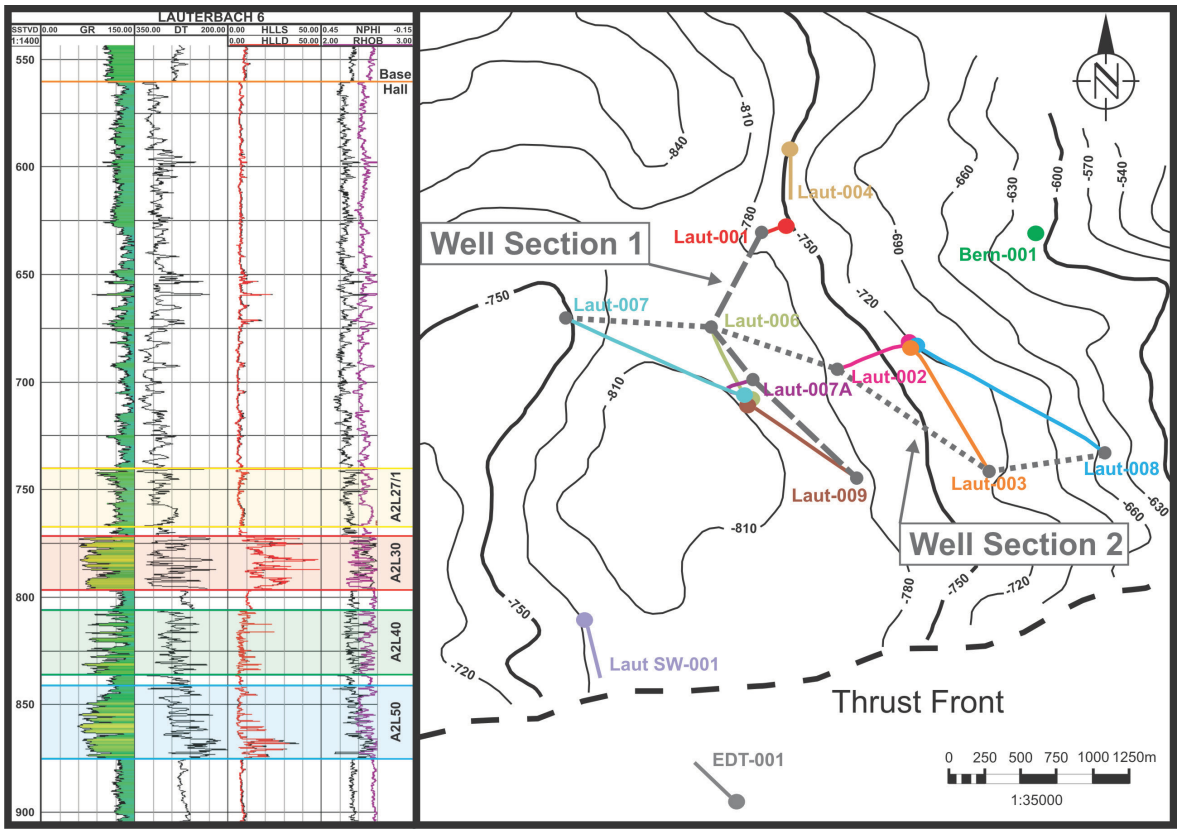

Fig. 18: Log-section of the reference well Laut-006 with defined reservoir zones and location of well sections 1 and 2

Characterisation of reservoir layers

Within the Lauterbach reservoir, five productive sand layers were encountered in the Upper Puchkirchen Formation. Correlatable characteristic log patterns were defined based on the reference well Laut-006. For orientation purposes, the horizon "Base Hall" is displayed in well section 1 (Fig. 24). The base of the Hall Formation represents the most prominent erosional surface in the Molasse Basin and is characterised by a sudden upwards decrease in the gamma log and an upward increase in sonic velocity.

A2L50:

The A2L50 interval represents the basal sand body deposited above the base of the Lauterbach Basin. In the central position of Lauterbach Basin (Laut-006, Laut-007A) it shows an egg-shaped log pattern, while in positions near or at the basin flanks thickness is decreased and the log pattern is not or only partially reflected. In the wells Laut-001 & Laut-009, the pattern is still recognisable, although the finer sediments at the base of the interval are missing. In the wells Laut-002, Laut-003 and Laut-008 the interval seems to appear in a completely different facies condition. This is a result of bidirectional sediment input. The sediment was mainly shed from a SSE direction for all productive sand layers, except for the interval A2L50, where an additional input direction from E is identifiable. This can be confirmed also by seismic data.

Due to this second input, that affected sedimentation in the eastern part of the basin, the A2L50 interval developed in a more fine grained condition compared to the a position in the centre of the basin, which can be clearly seen on the well logs of wells (e.g. Laut-003 in Fig. 19).

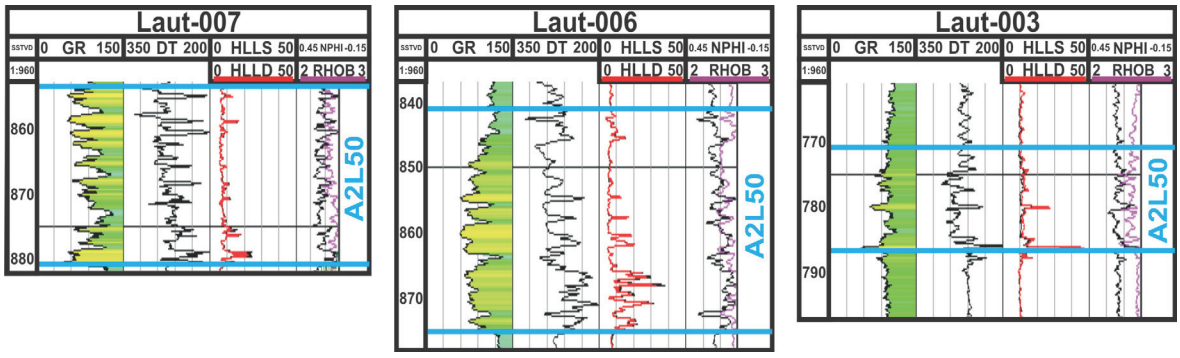

Fig. 19: Log patterns of the interval A2L50

Also the well Laut-007 shows a different log-pattern. This is a consequence of a different facies association. The interval A2L50 is primarily made up from sediments corresponding to FA 1 following the definition of Covault (2009). Laut-007 hits the interval in a position near the piggyback-basin margin, where the accumulation of FA 3 sediments is most likely to occur. Those chaotic mass sediments result in a serrated log pattern, showing no characteristic features like the egg-shaped pattern of the FA 1 in the basin centre.

A2L40:

The interval A2L40 was deposited above a shaly layer on top of the interval A2L50. It is characterised by an irregular serrated log pattern that shows a fining upward trend in some wells (Fig. 20). The thickness of the layer is relatively constant, except in the well Laut-001 where the thickness is decreased because of the exposed position of the well on the eastern basin flank. In the well Laut-007 it shows the same log pattern than the A2L50 interval, suggesting the same facies condition in this position: FA 3 following Covault (2009). Due to the fact that the interval is not present in a shallow depths on the eastern flank in the wells Laut-002, Laut-003 and Laut-008, similar to the A2L50 interval, it is located to a great extent below the GWC of the Lauterbach reservoir.

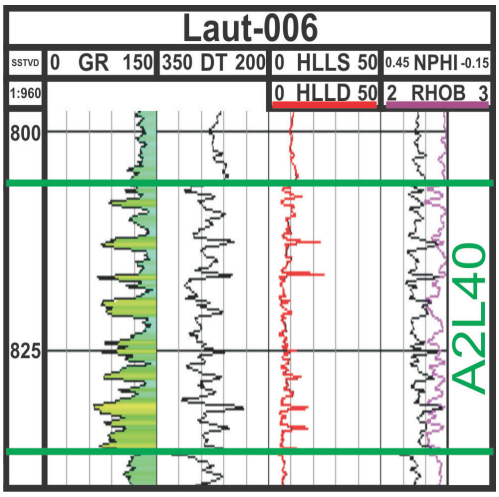

Fig. 20: Log pattern of A2L40

A2L30:

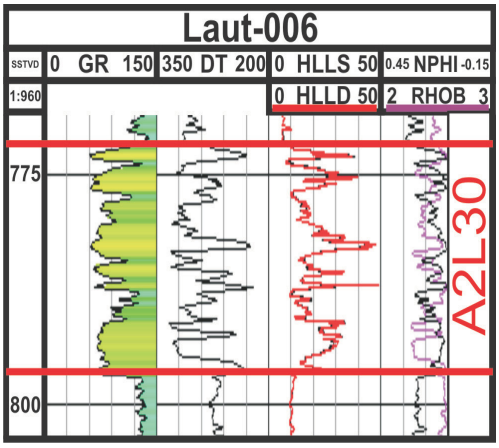

Fig. 21: Log pattern of A2L30

The interval A2L30 is the most promising layer with respect to reservoir properties of the reservoir section. Deposited with a thickness of up to 40 m and a high net to gross ratio it seems to provide best reservoir conditions. It is located above the GWC in all of the wells and shows a blocky log pattern (Fig. 21), in some wells with a shaly section in the upper part. The A2L30 interval

seems to be limited to the eastern part of the basin because the well Laut-007 did not encounter any sediment that would correspond to this layer. It is not present on the eastern basin flank either in the wells Laut-002, Laut-003 and Laut-008.

$A_2L_{27/1}$

Because the interval A2L27/1 was hit in just three wells the layer seems to be limited to the centre of the basin. It shows a characteristic coarsening upward trend (Fig. 22). Therefore the best reservoir conditions can be expected at the top of the section. Pressure data suggests at least a minor communication with the interval A2L30.

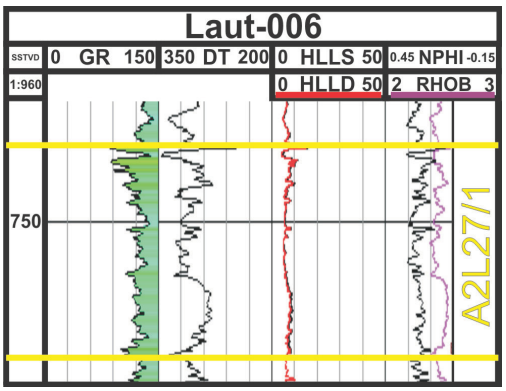

Fig. 22: Log Pattern of A2L27/1

$A_2L_{27/2}$

The uppermost reservoir layer, the A2L27/2 interval, was encountered only in the well Laut-009. Therefore a minor lateral extent is likely. It shows a serrated, blocky log pattern (Fig. 23). Communication might exist with the A2L27/1 interval.

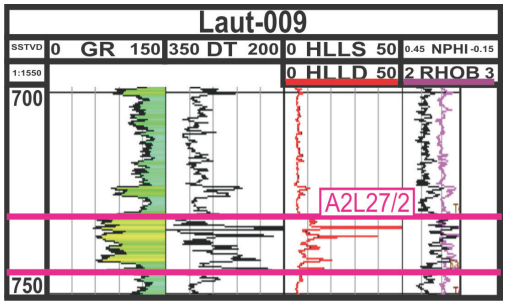

Fig. 23: Log pattern of A2L27/2

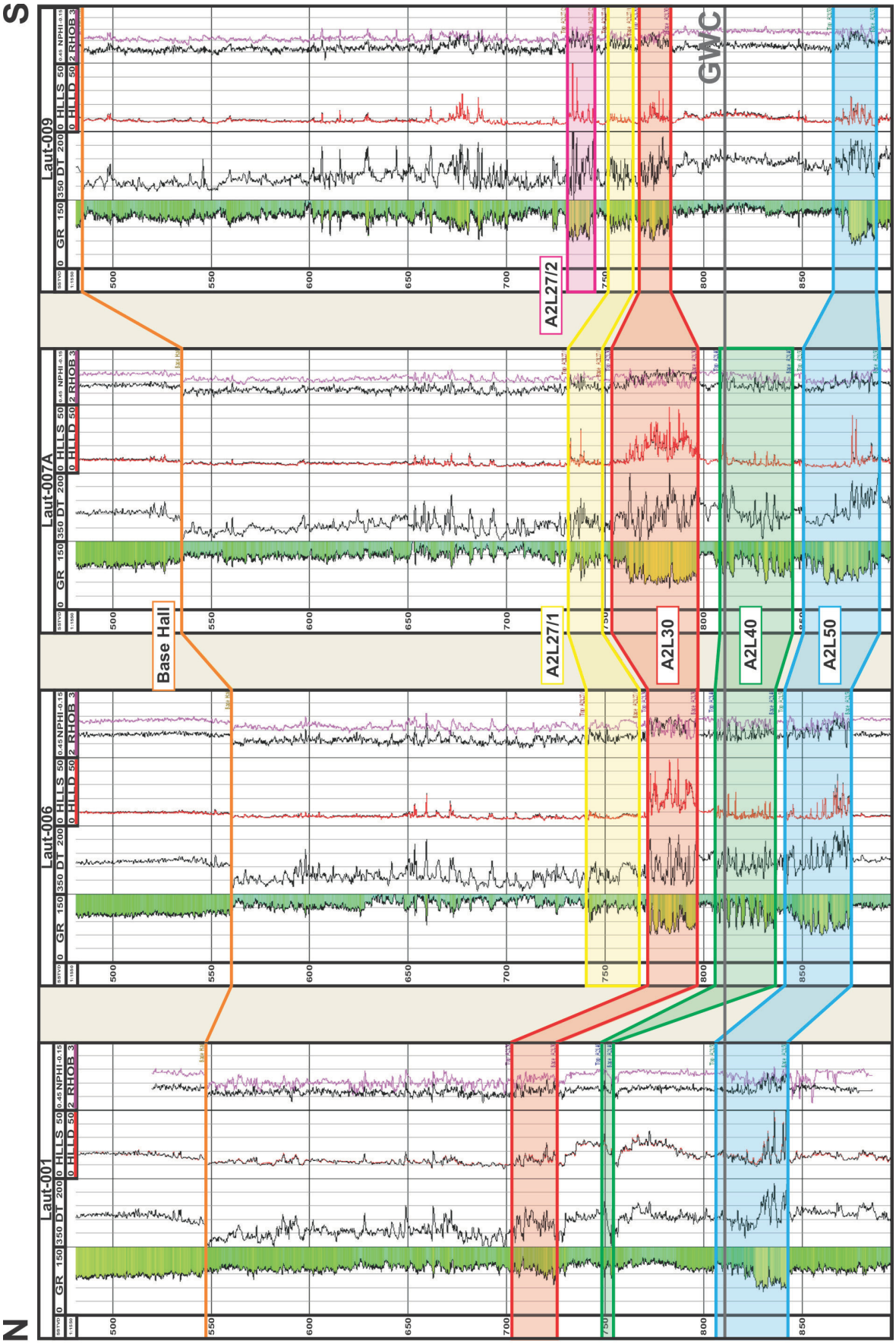

Fig. 24: Correlation of well section 1 (location of well section is shown in Fig. 18)

The correlation of the well logs was carried out with respect to reservoir units. This means that the correlation of reservoir units is not necessarily the same as the correlation of stratigraphic intervals, which is almost impossible to achieve when interpreting on a small scale like this in a rapidly changing depositional environment. Pressure data is the key element when defining which sections of one well communicate with sections in another well, although their log facies may vary significantly.

Apart from the well tops and thickness variations, which are both important inputs for seismic interpretation and modelling, both correlated sections (Fig. 24, Fig. 25) deliver some insights into the architecture Lauterbach reservoir:

1.) Beds are relatively constant in thickness and depth level in the centre of the basin, which is a consequence of the flat basin floor.
2.) Bed thickness is reduced significantly at the basin flanks.
3.) No other unit than the A2L50 interval is present on the south-eastern basin flank.
4.) Most of the reservoir units are encountered in the central part of the basin.
5.) Facies changes can occur abruptly, reservoir sands are spatially limited and do not cover the entire basin.
6.) The well Laut-007 shows an irregular serrated log pattern in all encountered reservoir units that does not fit with the patterns of the reservoir units in other wells.
7.) The base of the Lauterbach Basin is not recognizable in well logs, although seismic data indicates a position right below the A2L50 interval.
8.) Shaly sections with varying thicknesses separate the reservoir sands and prevent or at least reduce communication.

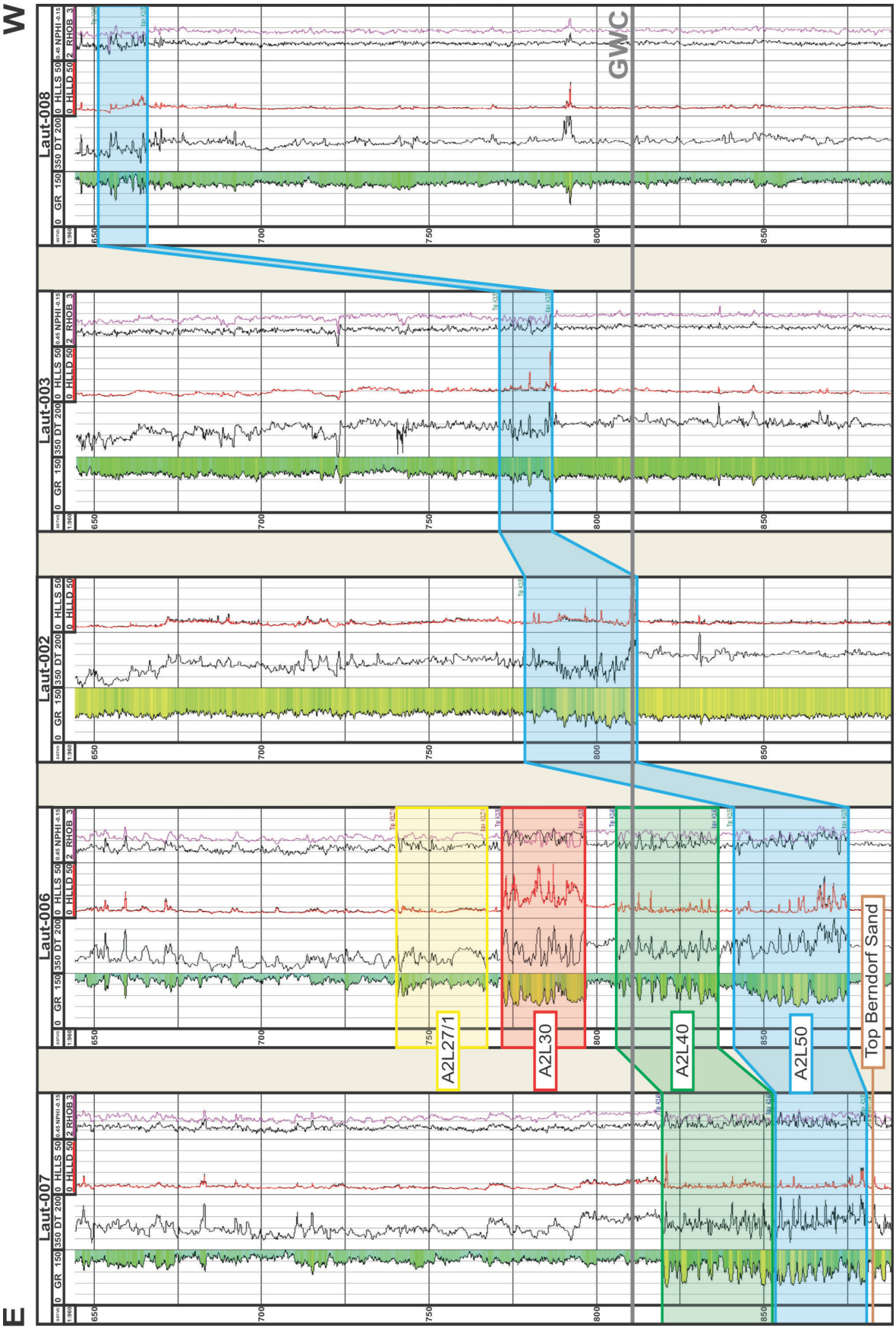

Fig. 25: Correlation of well section 2 (location of well section is shown in Fig. 18)

Seismic Interpretation

Seismic interpretation can be very challenging in a wedge-top environment. Erosive events, often smaller than seismic resolution, facies change and small bed thickness can easily result in misinterpretation. Therefore well-tops, defined in well correlation, form an essential base for a successful seismic interpretation. Reflectors often seem continuous, but are in fact the product of several lateral adjacent beds that feign the presence of one homogenous geologic unit. Changes in absolute amplitude values give hints in seismic interpretation. Geologic units also might extend further than their according reflector in the seismic data, but due to reduced thickness their signal can no longer be resolved separately.

In a setting like the Lauterbach Basin, where bed thickness is generally not much greater than seismic resolution, top and base of a reservoir unit cannot be determined separately. Well tops and synthetic seismograms (Fig. 26) help to identify reflectors that are suitable for the structural definition of the intervals of interest. In this case, after evaluation of well tops and synthetic seismograms, the reflectors were chosen to represent the top of the according reservoir layer.

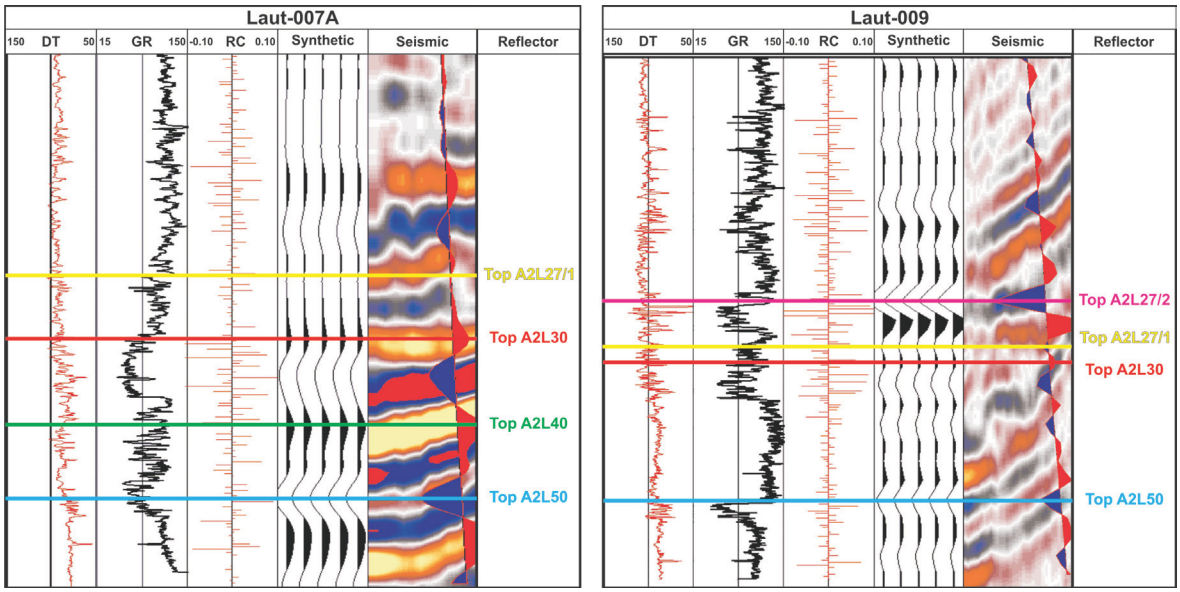

Fig. 26: Synthetic seismograms of wells Laut-007A and Laut-009 with definition of reflectors

The synthetic seismograms were generated using a “Reverse Ricker Wavelet”. This means that a negative reflection coefficient results in a peak (red colour) after convolution.

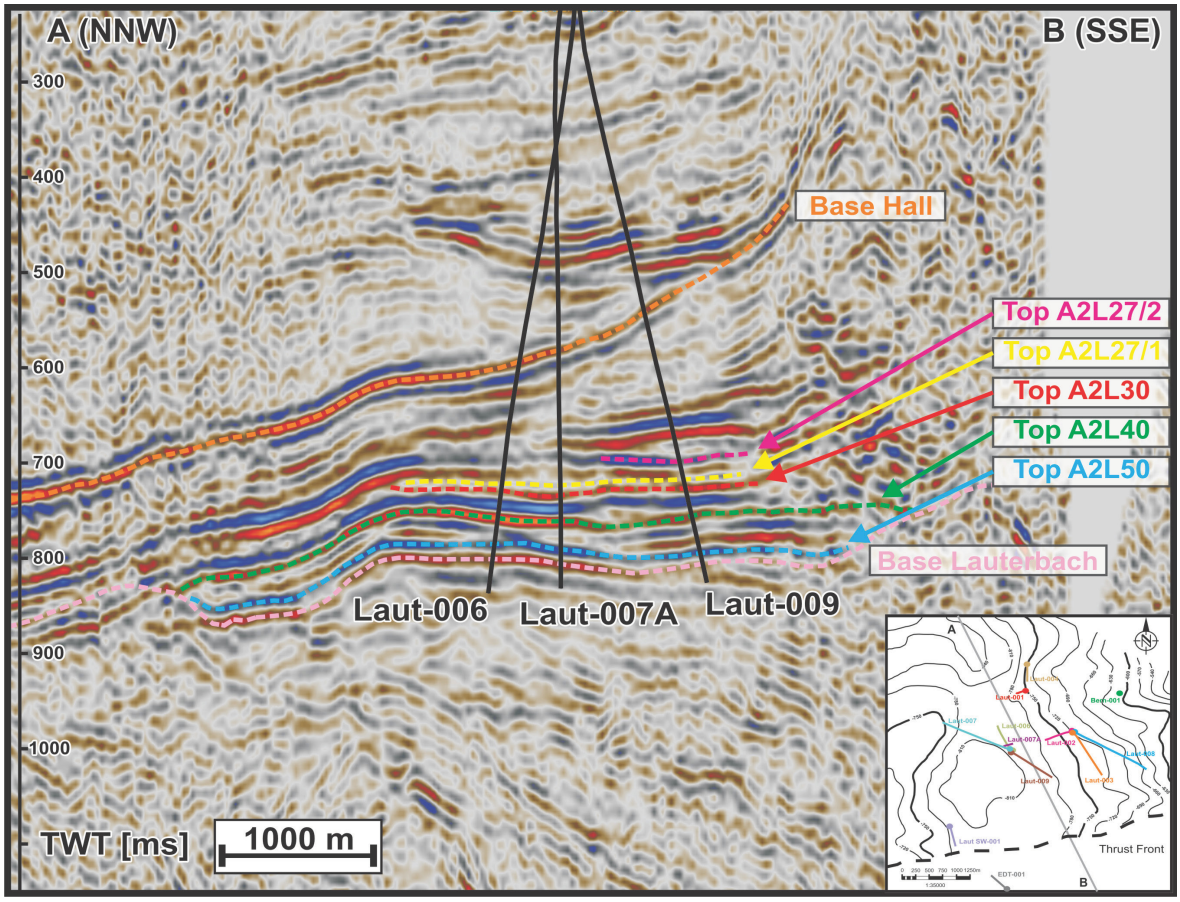

Fig. 27: Seismic cross section through the Lauterbach Basin

Several Horizons were interpreted with the aim to estimate the lateral extent of reservoir layers to define structural elements within the basin (Fig. 27, from base to top):

- Base Lauterbach
- Top A2L50
- Top A2L40
- Top A2L30
- Top A2L27/1
- Top A2L27/2
- Base Hall

Base Lauterbach

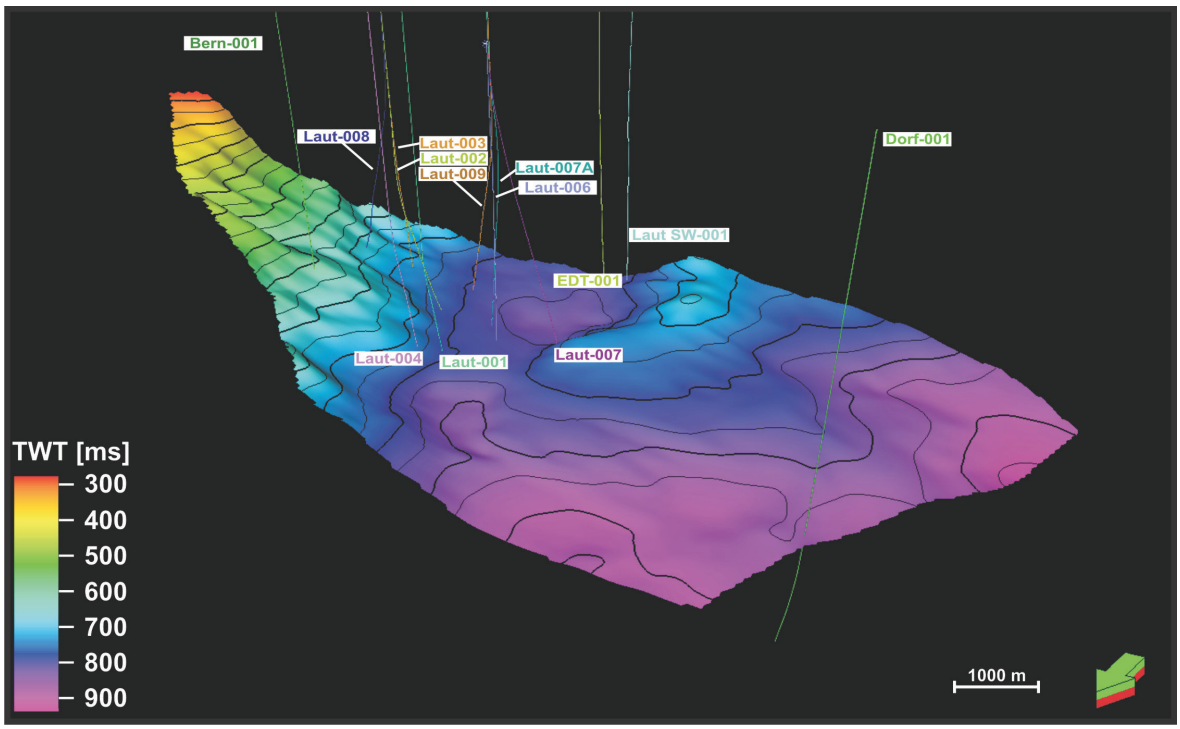

Fig. 28: Structural map of Base Lauterbach in TWT in 3D view

The base of the Lauterbach Basin is formed by a regional erosive even that cuts into a sedimentary succession ("Berndorf Sand") deposited on top of the Molasse Imbrications (Fig. 28). This succession was investigated by the wells Bern-001 and Dorf-001.

Mapping the top of the "Berndorf Sand" starting at the wells Dorf-001 and Bern-001 until it is cut by the Base Lauterbach erosive unconformity is a good support for the interpretation of the Base Lauterbach horizon, at least in the northern part of the study area. As indicated by the red ellipse in Fig. 29, the structural map of the Base Lauterbach horizon shows a swell zone (further referred to as "northern swell") in the northern part of the basin that forms a local barrier and divides the basin into two sub basins. It is unlikely that the erosive surface formed that way in first place. Therefore this structure is interpreted as an indication of syn-sedimentary deformation, related to movements of the underlying moving Molasse Imbrications.

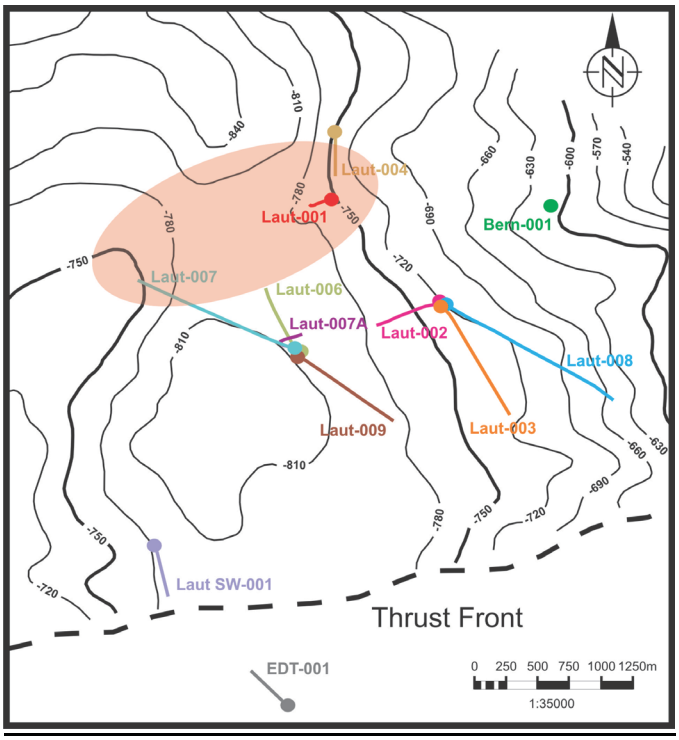

Fig. 29: Structural map of Base Lauterbach in TWT. The red ellipse indicates the position of the northern swell.

Top A2L50

The horizon Top A2L50 forms the first reflector on top of the Base Lauterbach horizon. It has the greatest lateral extend of all reservoir layers and shows continuous homogenous reflection characteristics.

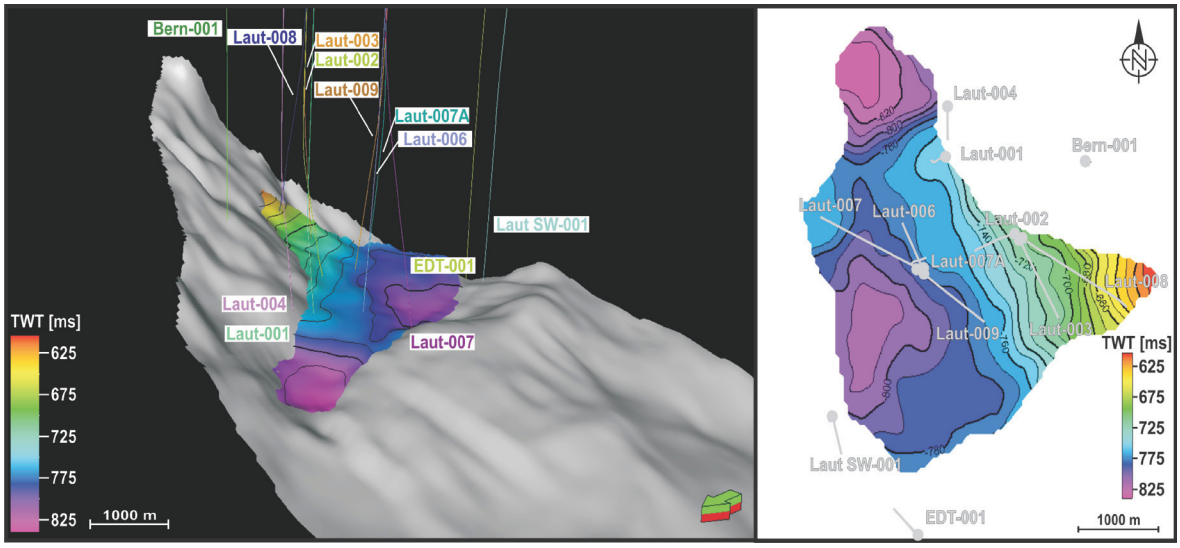

Fig. 30: Structural map of Top-A2L50 in TWT in 3D and 2D view. Base Lauterbach is underlain in grey in 3D picture.

As there can be seen in the structural map of the horizon in Fig. 30, sediments of the A2L50 interval extend on the eastern basin flank and are not limited to the deeper parts of the basin. As also seen in well correlation (Fig. 25), this is the result of an additional sediment input. Sediment was not only shed from SSE, which is the main sediment transport direction for the basin, but also from an eastern direction. The fact that only the horizon A2L50 shows such a characteristic feature, suggests that a massive short-time mass flow event rather than continuous sediment input led to the present sediment distribution. The lobe of the mass flow interfingers with the continuous turbidite input from SSE in the deeper depozone of the basin and forms one continuous reservoir layer with varying characteristics (Fig. 31).

The great areal extend of the layer, even past the northern swell to NNE, is a record of high turbiditic activity and therefore high sediment input in the basin (Fig. 30).

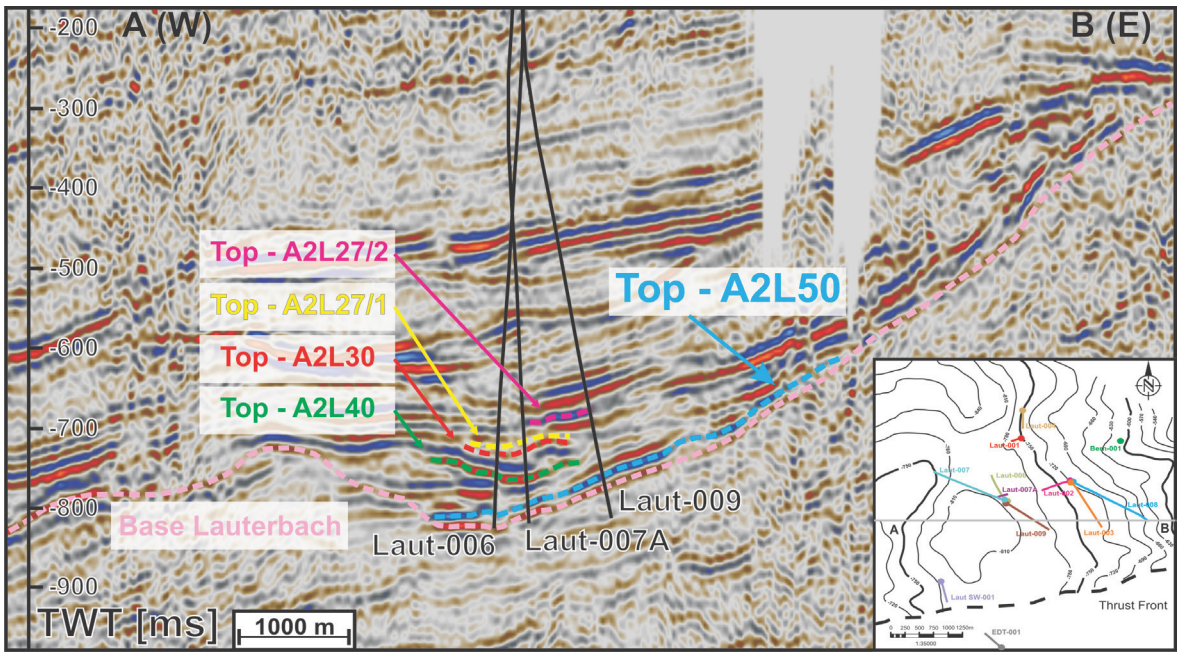

Fig. 31: W-E trending seismic cross section through the Lauterbach Basin showing the extent of the Interval A2L50 on the eastern basin flank.

Top A2L40

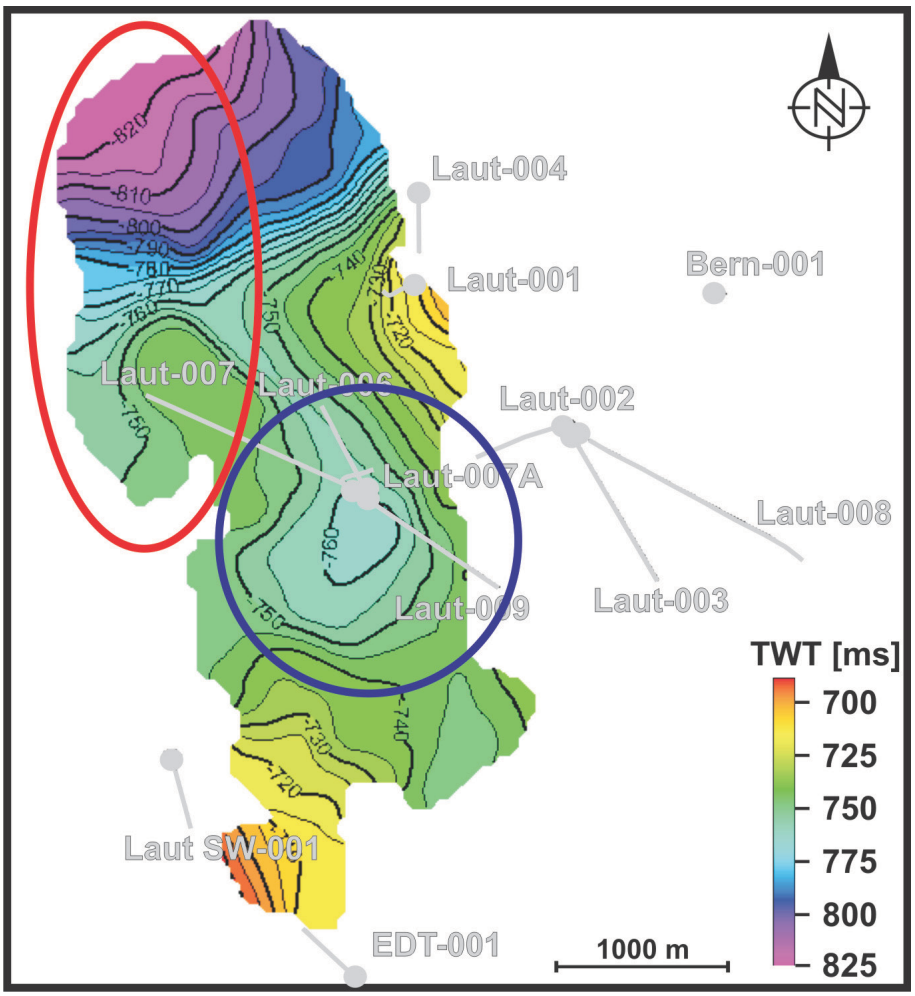

Fig. 32: Structure map of Top A2L40 in TWT

The structural map of the horizon Top-A2L40 shows that the lateral extent of this interval is limited to the centre of the basin. Although the sediments still reach past the swell zone into the northern sub-basin, where the reflector onlaps the Base Lauterbach horizon (Fig. 27) it does not cover the basin flanks, neither in the west nor in the east. The eastern input direction is not present or at least not in a structural important way like in the A2L50 interval. One interesting feature, highlighted by the red ellipse in Fig. 32, is the areal extent of the horizon into the north-western area of the study area, even further than the A2L50 interval, suggesting sediment input of at least the same intensity as in the underlying interval. The top of the A2L40 interval is defined by a major erosive event that indicates reduction in thickness of the interval. It is responsible for the structural low zone in the centre of the basin (blue circle in Fig. 32), a feature that influenced the geometry of younger reservoir layers.

Top A2L30

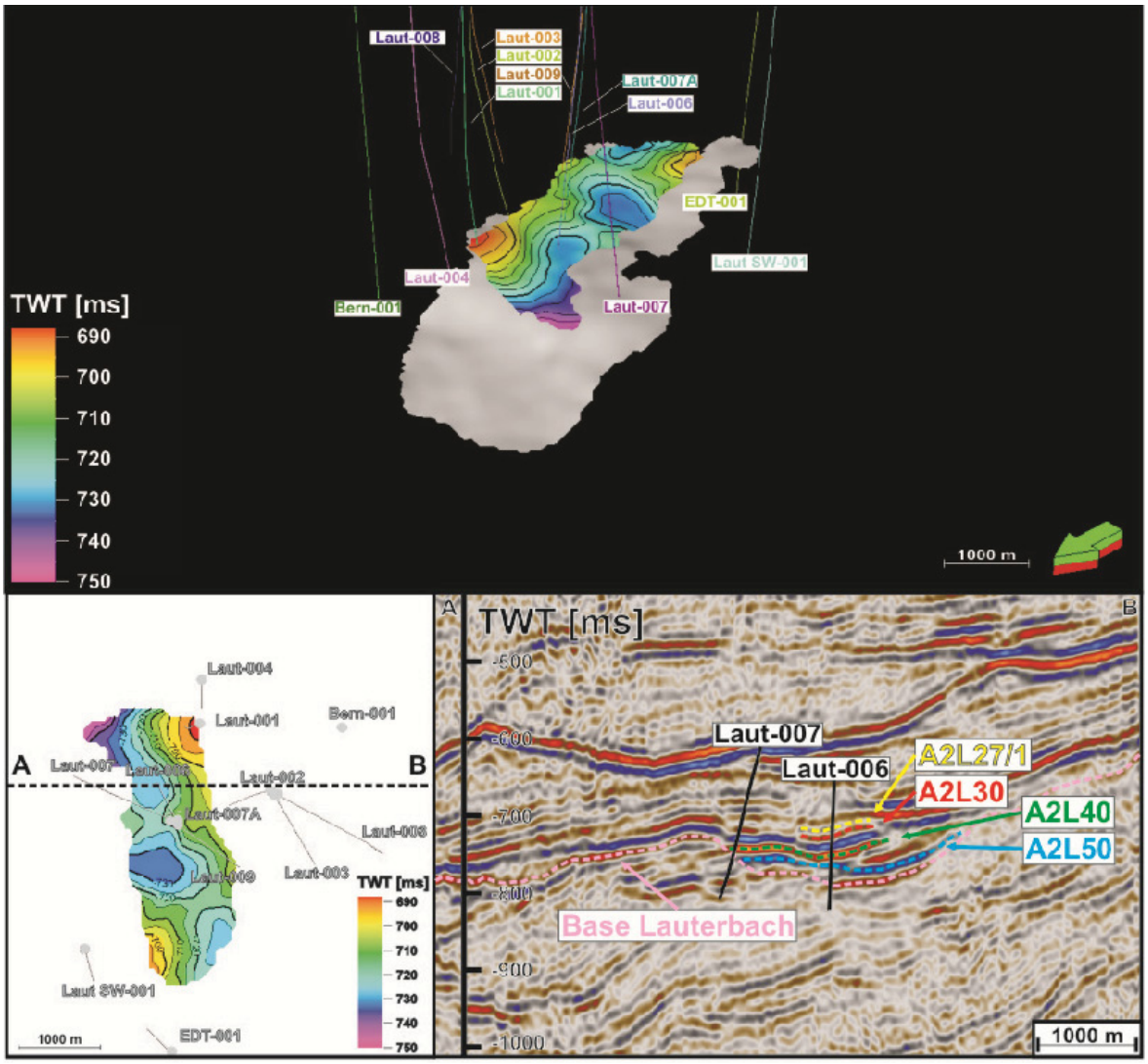

Fig. 33: Structural map of Top A2L30 in TWT in 3D and 2D view. The seismic cross section shows that the horizon does not extend into the western part of the basin.

The Horizon Top-A2L30 is limited to the centre of the basin and does not reach past the northern swell. Although reflection seems to be continuous the interval is not present in the western part of the basin, where the well Laut-007 was drilled into (Fig. 33). This is a result of the morphology that was generated by the erosive event that defines the top of the A2L40 interval (Fig. 34). It channelized sediment transport to the centre of the basin that provided space for sediment accumulation. Thus, the western part of the basin was cut off from sedimentation.

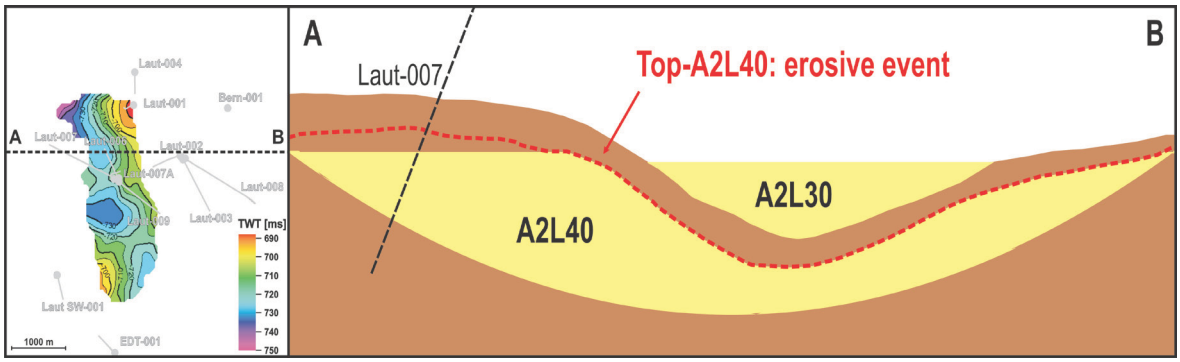

Fig. 34: Schematic reconstruction of deposition of the A2L30 interval

Top A2L27/1 & Top A2L27/2

Both intervals are poorly resolved in seismic data. The reflection amplitudes are low and not good in contrast, compared to the other interpreted horizons due to the reduced thickness. Both intervals are limited in their lateral extent, suggesting minor sediment input (Fig. 35). This is also confirmed by the limited number of wells that encountered these intervals. The top of the interval A2L27/1 is defined by another major erosional event.

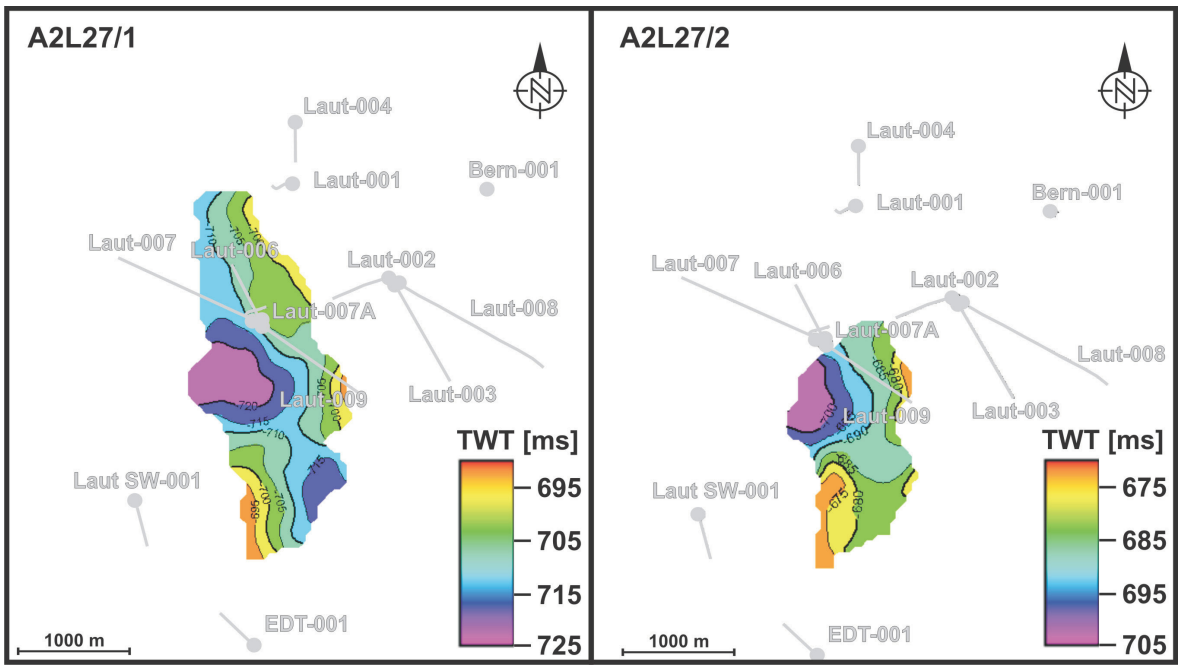

Fig. 35: Structure map of Top A2L27/1 and Top A2L27/2 in TWT

Time/Depth Conversion

After seismic interpretation, the next step is to convert the mapped horizons into the depth domain. This was achieved by a procedure that has delivered good results in the past in the study area. It is based on calculating average velocity surfaces from SRD (Seismic Reference Datum; 300m above sea level) to a certain reflector. In this case, two velocity surfaces were calculated to achieve an accurate result.

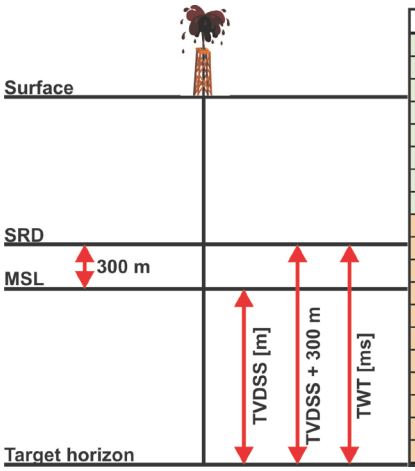

Well	Top	TVDSS	TWT (picked)	Avg. Vel. SRD - Top
EDT-001	Top_A2L30	767,61	695,64	3069,43
Laut-001	Top_A2L30	702,91	700,73	2862,47
Laut-002	Top_A2L30	702,92	684,64	2929,77
Laut-006	Top_A2L30	771,91	728,5	2942,79
Laut-007	Top_A2L30	771,81	709,2	3022,59
Laut-007A	Top_A2L30	753,72	727,77	2895,75
Laut-009	Top_A2L30	767,5	709,65	3008,53
Laut SW-001	Top_A2L30	767,61	691,82	3086,38
EDT-001	Top_A2L50	869,76	751,86	3111,64
Laut-001	Top_A2L50	809,34	766,01	2896,41
Laut-002	Top_A2L50	780,33	754,49	2863,74
Laut-003	Top_A2L50	773,96	715,91	3000,27
Laut-004	Top_A2L50	809,3	747,67	2967,35
Laut-006	Top_A2L50	847,63	780,8	2939,63
Laut-007	Top_A2L50	853,65	763	3023,98
Laut-007A	Top_A2L50	848,24	783,5	2931,05
Laut-008	Top_A2L50	654,75	660,91	2889,20
Laut-009	Top_A2L50	869,91	771,81	3031,60
Laut SW-001	Top_A2L50	869,76	752,66	3108,34

Fig. 36: Sketch illustrating time/depth relation. The table on the right summarizes input data for T/D conversion.

At first TVDSS (True Vertical Depth Sub Sea) and TWT (Two Way Traveltime) of well tops of the according horizons, in this case Top A2L30 and Top A2L50, have to be evaluated (Fig. 36). With this data, average velocity from SRD to the well top of the horizon can be calculated using the simple path-time relationship:

$$Avg.Vel. = \frac{x}{t} = \frac{2000 * (TVDSS + 300)}{TWT}$$

The factor 2000 in the formula is needed to convert the TWT into a one way traveltime in seconds from SRD to the desired horizon. This formula is applied to every well that penetrated the horizon. As additional input artificial well tops at adjacent wells that did not encounter the horizon can be generated, so that velocity trends can be analysed in a more representative way.

The result of the before described procedure is an average velocity point dataset that has to be interpolated to get a velocity surface that allows the interpretation of velocity trends and the depth conversion of seismic horizons.

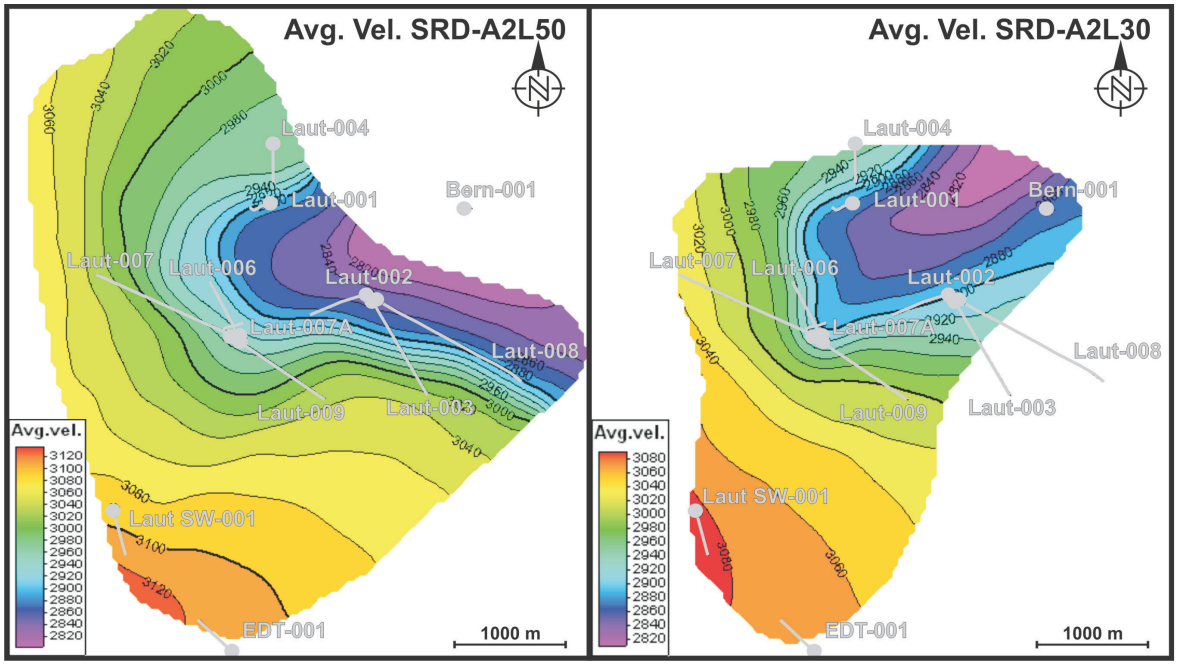

Fig. 37: Average velocity maps for the horizons Top A2L50 and Top A2L30

In this case, two surfaces were generated (Fig. 37). The surface SRD-A2L50 was used for depth conversion of the horizons Top-A2L50 and Top-A2L40 and the surface SRD-A2L30 was used for Top-A2L30, Top-A2L27/1 and Top-A2L27/2. It is not necessary to calculate a velocity surface for every mapped reflector, because velocity variations are not significant when the reflectors are close to each other. It is very important that the velocity surface is bigger in lateral extend than the mapped horizon, otherwise the multiplication of those two elements will result in strange results.

Now that velocity surfaces are generated, the horizons can be converted into depth domain by the following two steps:

1.) $horizon\ [depth] = horizon\ [time] * average\ velocity\ surface$

2.) $horizon\ [depth] = \frac{horizon\ [depth]}{2000} + 300$

The second formula is necessary two set depth interval to meters and shift the horizon back to its original position with respect to SRD.

3D – Geologic Modelling

Before the modelling process begins, it is essential to summarize the results of well correlation and seismic interpretation and evaluate them with respect to the geologic context. This is the first and most important step on the way to a representative and accurate geologic model. The second step is to find a way to fit the geologic setting into a simulatable static 3D model.

Fig. 38 shows the evolution of the Lauterbach Basin with the help of a simplified SSE-NNW trending cross section:

1.) Basin evolution started with an erosive event that cut into sediments on top of the Molasse Imbrications ("Berndorf Sand") and formed the base of the Lauterbach Basin.
2.) While the sedimentation of the interval A2L50 and A2L40 took place, stress from the underlying Molasse imbrications led to structural deformation of the basin and the deposited sediments. The northern swell and the northern basin margin were formed. A major erosive event formed the top of the A2L40 interval that is still influenced movements of the underlying Molasse Imbrications. This can be deducted from the observation that the morphologic high of the northern swell is still recognizable.
3.) The intervals A2L30 and A2L27/1 were deposited in the southern part of the basin and lap onto the morphologic high above the northern swell. Another major erosive event cut into the sediment succession: the Top-A2L27/1 erosion that shows no signs of tectonic deformation.
4.) Thereafter, the interval A2L27/2 has been deposited in the southernmost part of the basin.

Using this simplified history of the Lauterbach Basin, the present day situation evaluated from seismic data can be explained. As there is was no well drilled into the northern part of the basin, there is no detailed information available on the deposits in this area (indicated by the question mark in Fig. 38, 4).

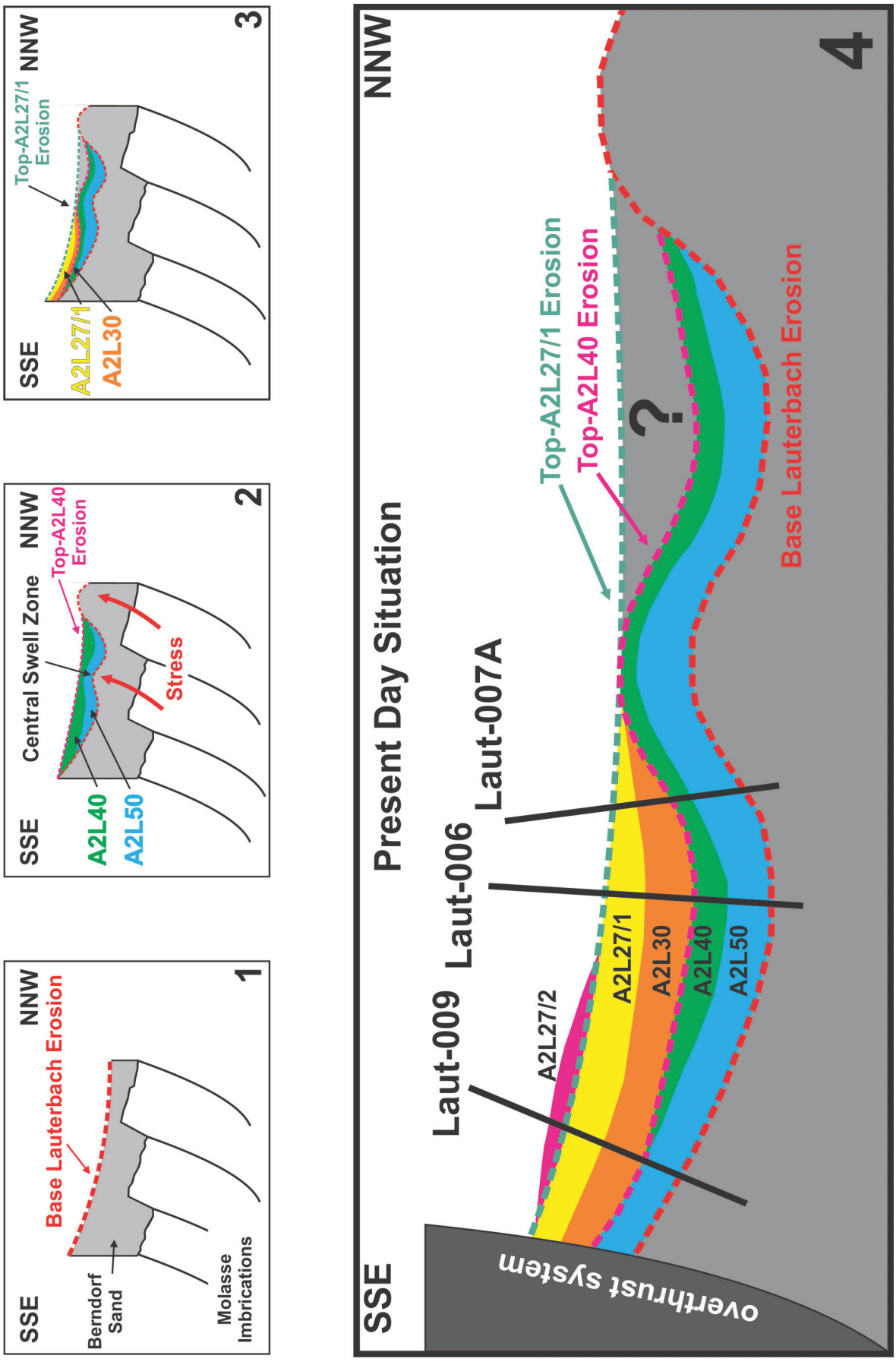

Fig. 38: Sketch illustrating the development of the Lauterbach Basin (simplified)

Geometric Modelling

The first step in the modelling process is to define geometries of reservoir layers and the sediments in between. The top-horizons were interpreted and converted to depth. The next problem is how to define the base of the reservoir layers that is not mappable in seismic data. Therefore the base surface has to be generated artificially. This was achieved by the means of thickness maps for each reservoir layer.

Thickness Maps

Generating thickness maps with nothing than the well tops of several wells is not representative and therefore not sufficient to define the base surface. Seismic attributes should deliver the needed trends in thickness distribution. Amplitude variations can not only be used for the evaluation of the media present in the pores, but also for the estimation of bed thickness. With bed-thickness in the range or below seismic resolution, the seismic amplitude is likely to be a consequence of thin layer interference. Therefore, the reflection amplitude is related directly to layer thickness, increasing monotonically from zero at zero layer thickness to a maximum at tuning thickness (Robertson, et al., 1984; Gochioco, 1991; Chadwick, et al., 2004).

As mentioned before, amplitude variations can also be indicative for the change of the pore fluid or facies change, generally for a variation of acoustic impedance. When the GWC of a reservoir is known amplitudes below and above the contact can be analysed and compared. In the Lauterbach Field this led to the result that the pore fluid has a minor influence on the amplitude intensity. Therefore facies change and bed thickness seem to be the controlling factors.

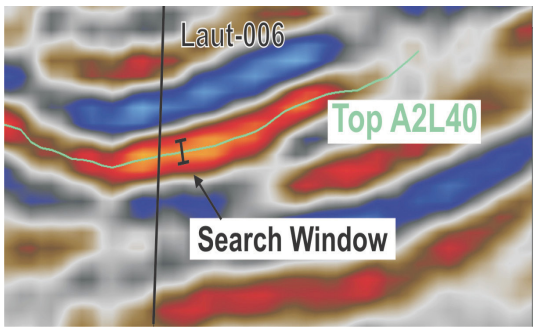

Fig. 39: Size of search window for RMS amplitude extraction

The attribute shown in the following maps is the RMS amplitude with a search window of 3ms below and above the interpreted horizon (Fig. 39). For the generation of thickness maps those RMS amplitudes were scaled to the values 0 for minimum and 1 for maximum and used as trend surface in thickness distribution.

As shown in Fig. 40, the thickness maps were generated using the following steps:

1.) *Definition of layer boundary*

For each interval the outline of the mapped seismic horizon was digitized. This polygon was defined as the line of pinch out of the zone and the thickness was set to 0.

2.) *Well data input*

The thickness of each reservoir layer is known at the well location. Therefore these thickness values were extracted and used as point data input set.

3.) *Scaled amplitude trend surface*

Those surfaces were used to define a trend in thickness variation. The scaling from 0 to 1 is needed to achieve a representative trend for all layers.

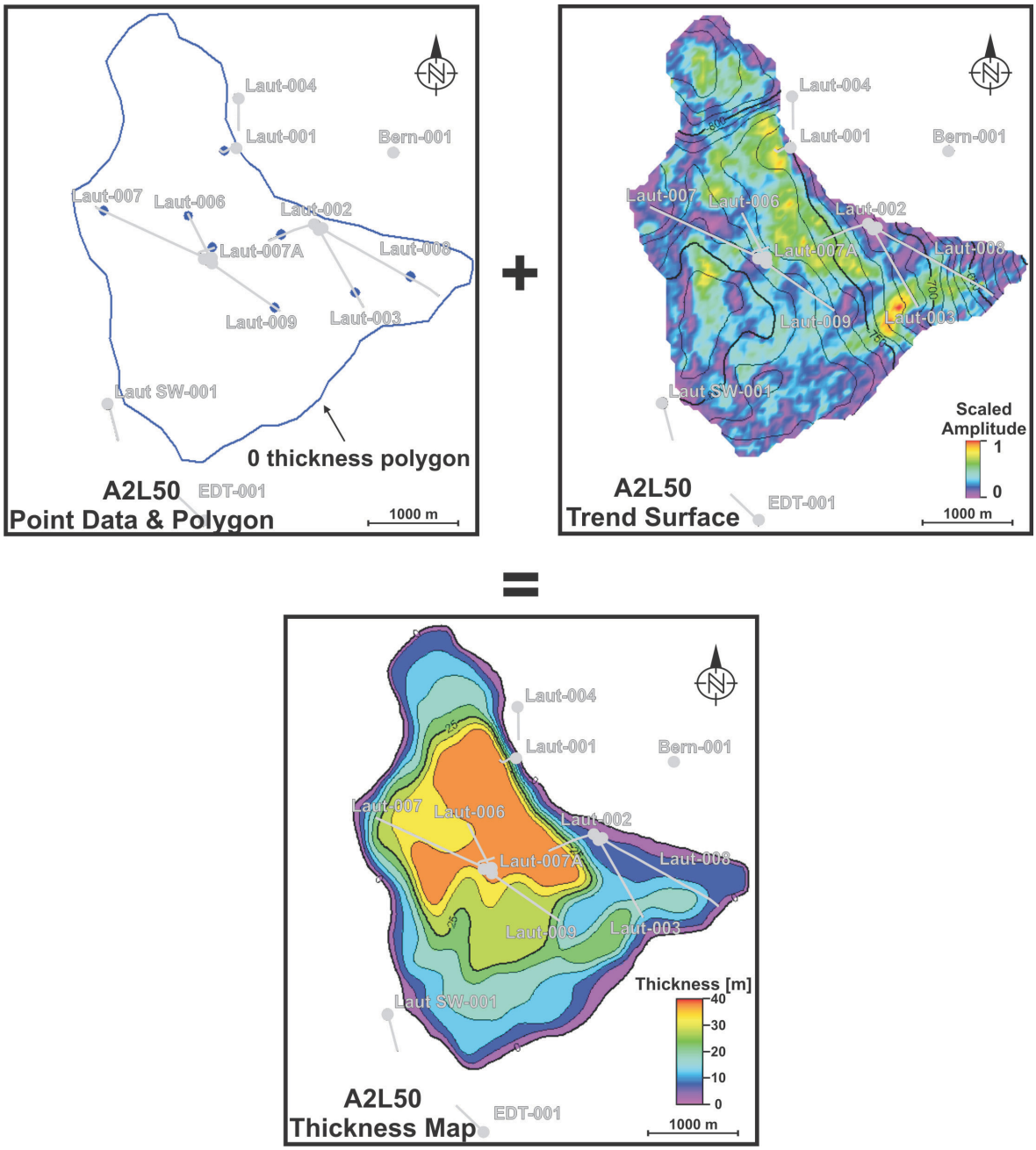

Fig. 40: Generation process of thickness maps

The steps considered to go from thickness maps to maps of the base of the horizon are shown in Fig. 41 and essentially comprise the addition of the layer thickness to the top of the horizon.

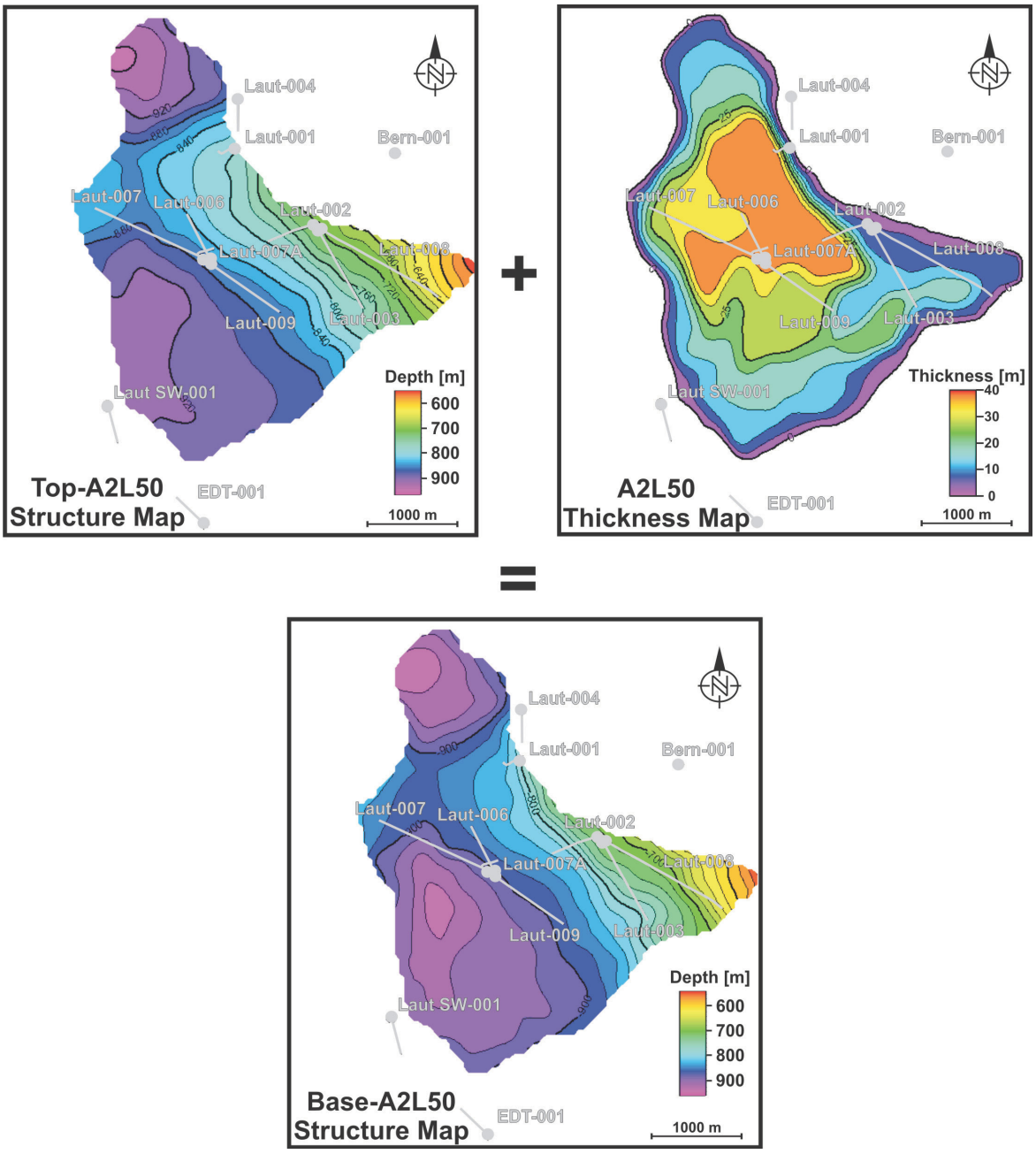

Fig. 41: Generation process for base horizon for the interval A2L50

The procedure shown in Fig. 41 for the example of the A2L50 horizon was carried out for each layer in the reservoir.

Gridding and Layering

Gridding and layering is the next step in definition of the reservoir geometry. It defines the number and the volume of the cells of which the model consists and that can be filled with various properties. The essential question in this step is: how much detail should be resolvable in the geologic model, also with respect to a later dynamic reservoir simulation?

This has to be considered in lateral as well as in vertical direction. Lateral resolution is dependent on the size of the reservoir itself. In this case a grid cell size of 100 x 100 m is suitable to reflect all features of the reservoir in the desired detail.

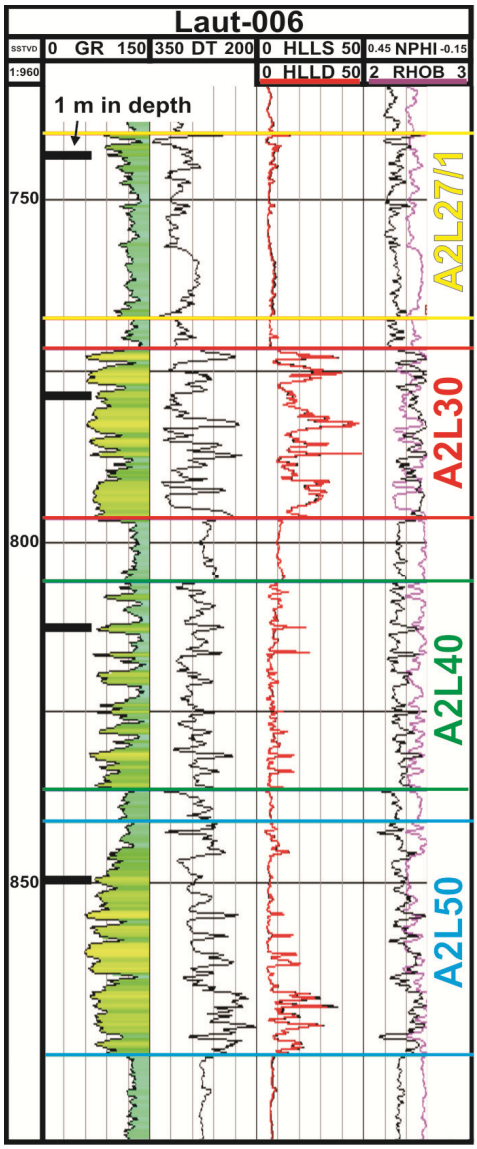

The thickness of the grid cells is dependent on the thickness of sand layers within the separate reservoir zones and can vary from zone to zone. It can be reasonably estimated by the use of well logs. In Fig. 42, the depth interval of 1 m is represented by the black rectangle that is shown in each reservoir section. This seems to be a good fit for the zones A2L50, A2L40 and A2L30 because the sand layers are generally thicker than 1 m. For the section A2L27/1 and also for the section A2L27/2, that was not encountered in the well Laut-006, a layering of 1 m would not reflect the details of the reservoir zone because the sand layers are thinner than 1 m. As a consequence, the height of the grid cells was set to 0.5 m in the two uppermost layers.

Fig. 42: Illustration of definition of cell height with respect to layer thickness in reservoir zones

Between the reservoir zones, sediments that limit or prevent communication between those zones were deposited. Therefore they have to be considered with respect to a later dynamic reservoir simulation. Those barrier zones were modelled as homogeneous volumes that form the matrix in which the closed volumes of productive zones were imbedded. They are represented by the grey zones in Fig. 43.

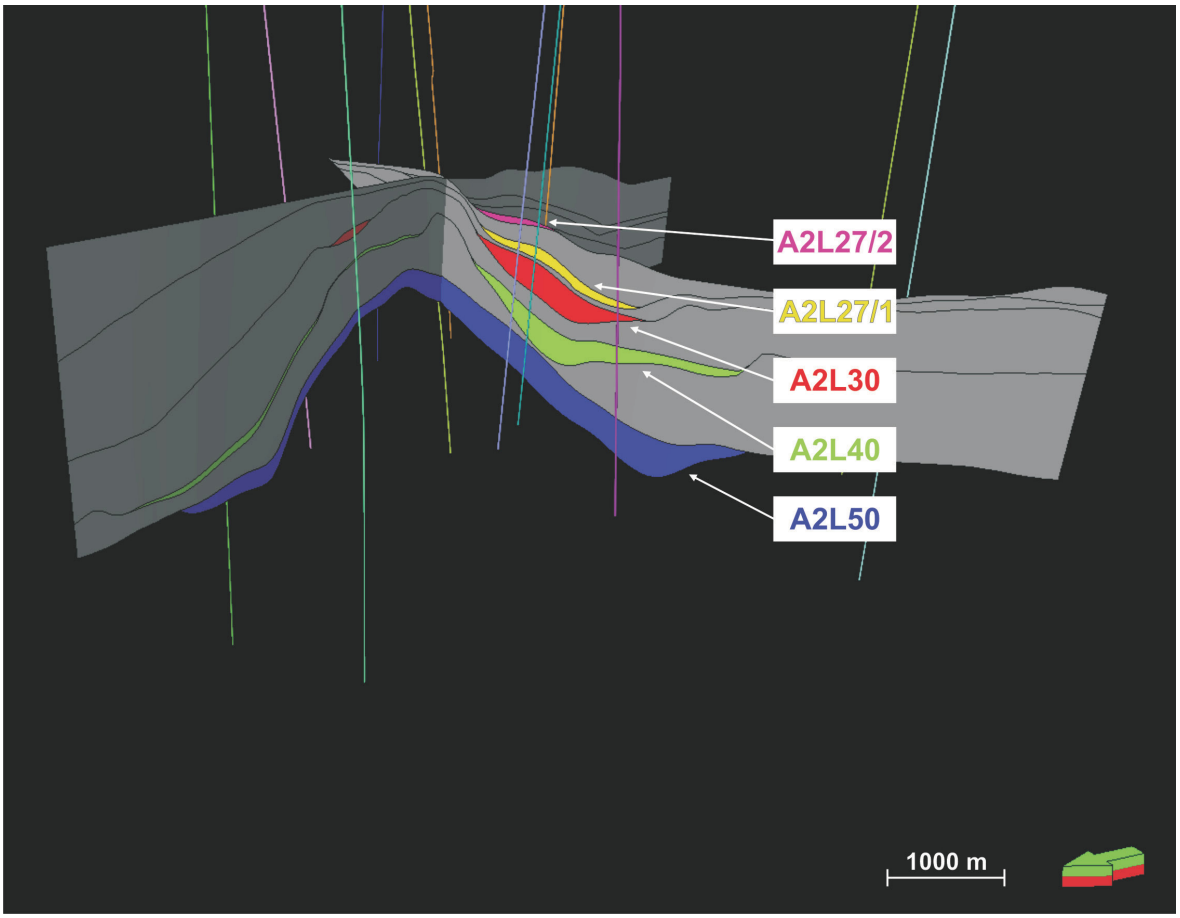

Fig. 43: 3D view of modelled zones in the Lauterbach Basin

Facies Modelling

With the geometries defined, it is necessary to find a way to distribute properties throughout the reservoir. This can be achieved by a stochastic distribution method that fills the cells in the model with values based on a geostatistic function or by a more sophisticated method that takes into account the depositional environment and sedimentary processes. This method is referred to as facies modelling and is based on the one hand on the definition of facies zones and on the other hand on the implication of geobodies (e.g. channels, lobes) in the environment of deposition. The process is based on a detailed analysis of the input data for the model and identifiable trends extracted from them.

Mutti (1985) described a turbidite system that shows the characteristics of relatively small sand filled channels with fine grained overbank deposits (Fig. 44).

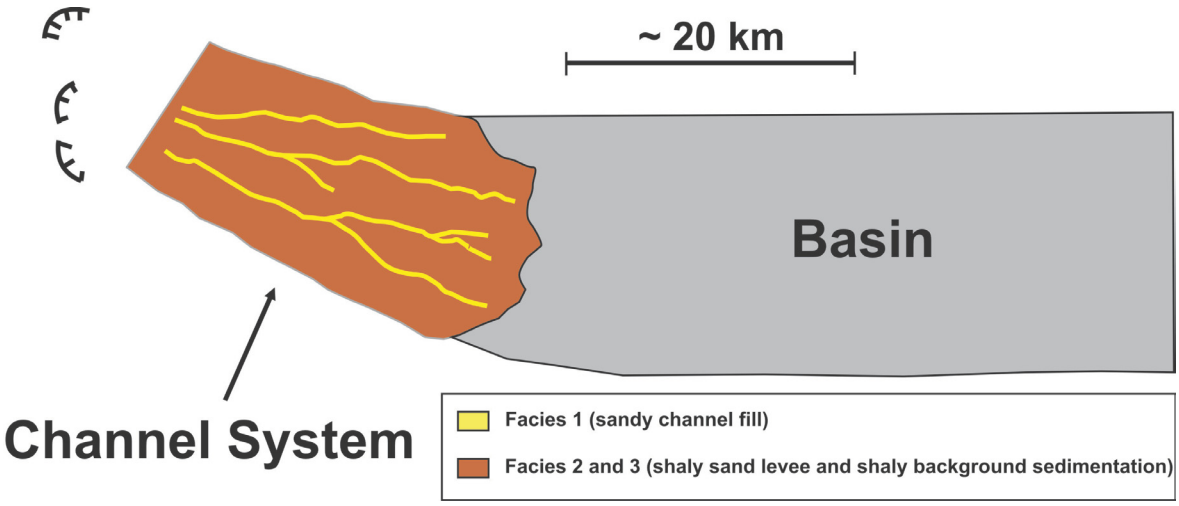

Fig. 44: Sketch illustrating turbidite system development, modified from Mutti (1980)

In this setting, aggradational background sedimentation is punctuated by debris flows or turbidites that show erosional surfaces at their base, resulting in a complex channel-levee architecture (Dade, et al., 1994; Morley, et al., 2008). This turbidite model forms the base for the geometries used in the facies model of the Lauterbach Basin. Core data analysed from Covault (2009) forms the most important input for finding an appropriate turbidite system model, because seismic data alone is not sufficient to interpret depositional facies in a turbidite system (Shanmugam, 2002).

Definition of Facies Zones

The first step on the way to a representative facies model is the definition of facies zones. In the case of the Lauterbach reservoir, three facies zones were defined:

1.) *Sandy Facies*

This zone represents the productive turbiditic sand layers with good porosity and permeability that form the fill of the channels formed in turbiditic events.

2.) *Shaly-Sand Facies*

Minor porosities and permeabilities are present throughout this zone that represents the fine grained parts of turbidites in combination with background sedimentation deposits.

3.) *Shaly Facies*

This facies zone reflects the background sedimentation between turbiditic events. No porosity or permeability is present in this facies zone.

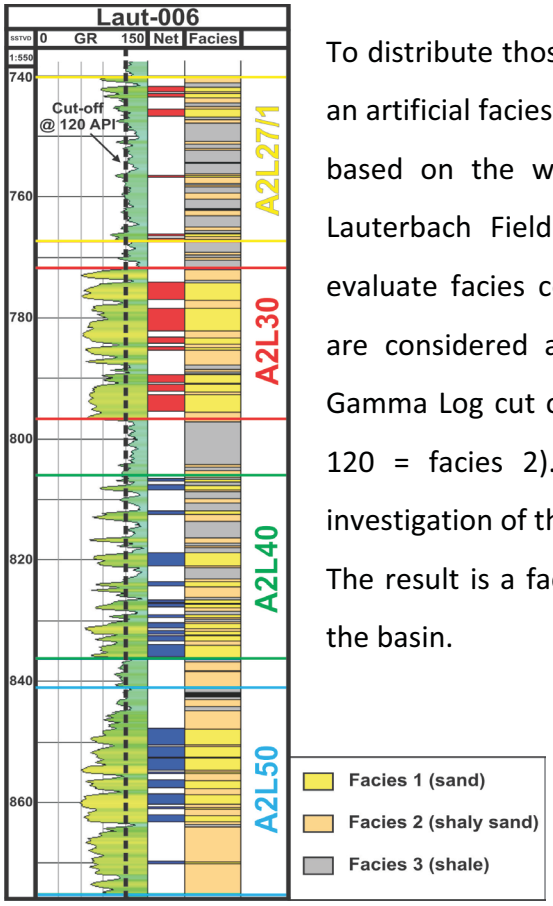

To distribute those facies zones throughout the reservoir model, an artificial facies log for the zone of interest has to be generated based on the well logs that are available (Fig. 45). For the Lauterbach Field the Gamma Log is an appropriate tool to evaluate facies conditions. Known net thicknesses in the wells are considered as facies 1, facies 2 and 3 are defined by a Gamma Log cut off value of 120 API (GR > 120 = facies 3, GR < 120 = facies 2). The cut off value is based on a detailed investigation of the Gamma Logs of all wells in the study area.

The result is a facies log that can be calculated for each well in the basin.

Fig. 45: Log section of reference well Laut-006 showing the determination of the facies log

Upscaling of Well Logs

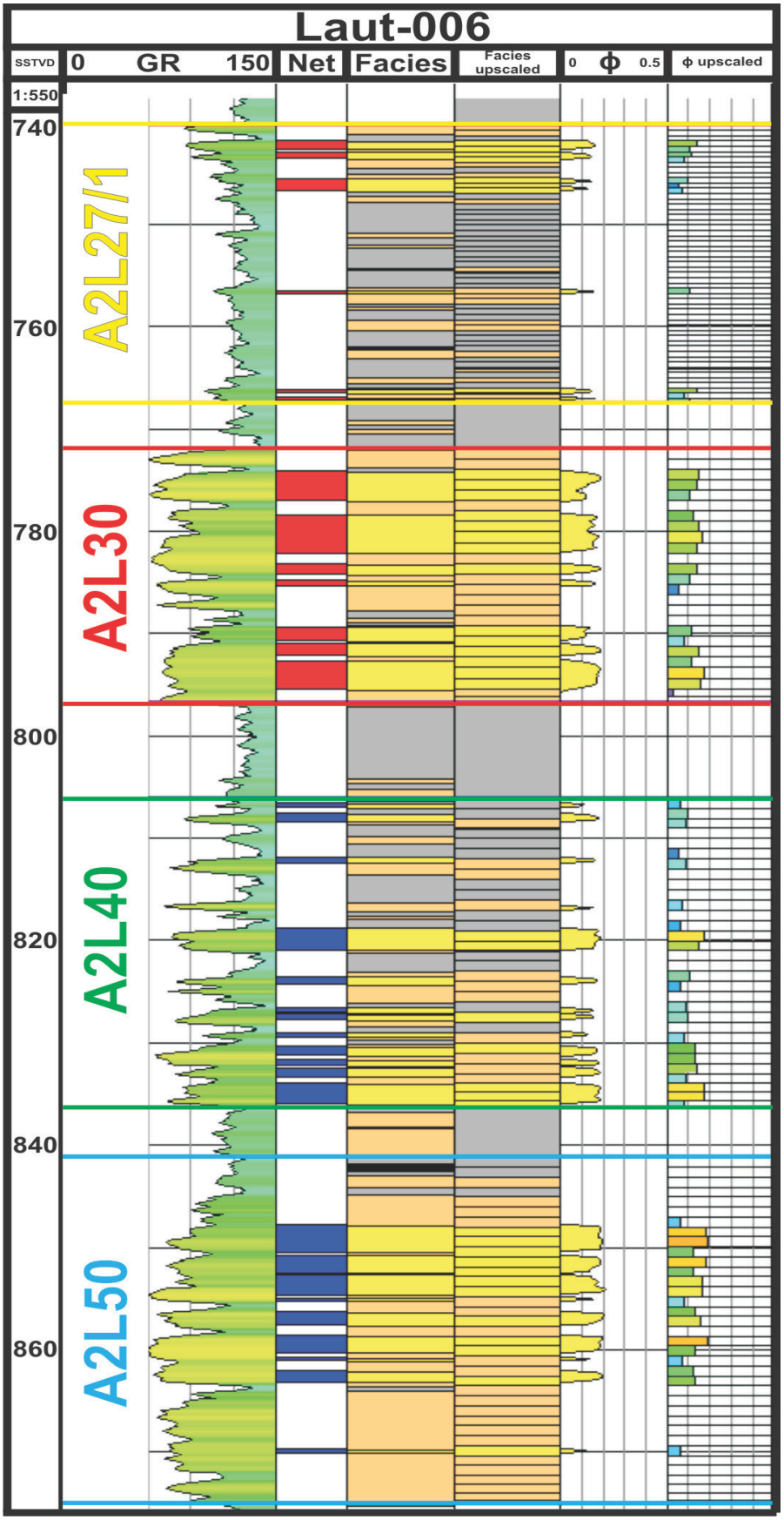

Fig. 46: Upscaling of well logs shown for the reference well Laut-006

The logs needed for distribution of reservoir properties have to be upscaled to the cell size of the geometric model. According to the layering this means 1 m intervals for the zones A2L50, A2L40 and A2L30 and 0.5 m for the zones A2L27/1 and A2L27/2.
Upscaling is a tricky process, because the upscaled log must still reflect the original log in terms of trends and values. In this case the best fit was achieved by a method that is called “Mid-Point Pick” where an interval of the upscaled log is filled by the value of the original log that is situated in the centre of the upscaled zone.

As shown in Fig. 46, not only the facies log was upscaled, but also the porosity log provided by RAG. The RAG porosities were in this case calculated only for the net intervals of the reservoir zones, therefore porosities had to be estimated for the facies zone 2.
In the upscaling process, the facies of the barrier layers between the reservoir intervals was set to shale (no porosity) to prevent communication between the layers in a dynamic simulation. This can be changed easily and therefore a mechanism for on-/off switchable communication between the reservoir intervals was incorporated in the model.

Data Analysis

The uspcaled cells along the boreholes of the wells can be analysed to extract trends in vertical direction for facies propagation throughout each separate reservoir layer. This means in detail that for each layer within the reservoir zone a probability can be defined at which a certain facies will be set in the cell. Those probability curves are a powerful tool. Therefore it has to be made sure that the extracted trend is representative. The more wells encounter a certain interval, the more cells can be taken into account and the more representative the vertical distribution function will be.

As an example, the definition of the vertical probability curve is shown for the interval A2L30 with its high net to gross ratio (Fig. 47). Therefore the probability for facies 1 is relatively high throughout the whole interval.

Trends can also be set in lateral direction, with the aim to model sediment input direction in the right way. The input direction from SSE is taken into account for the later distribution in the geologic model.

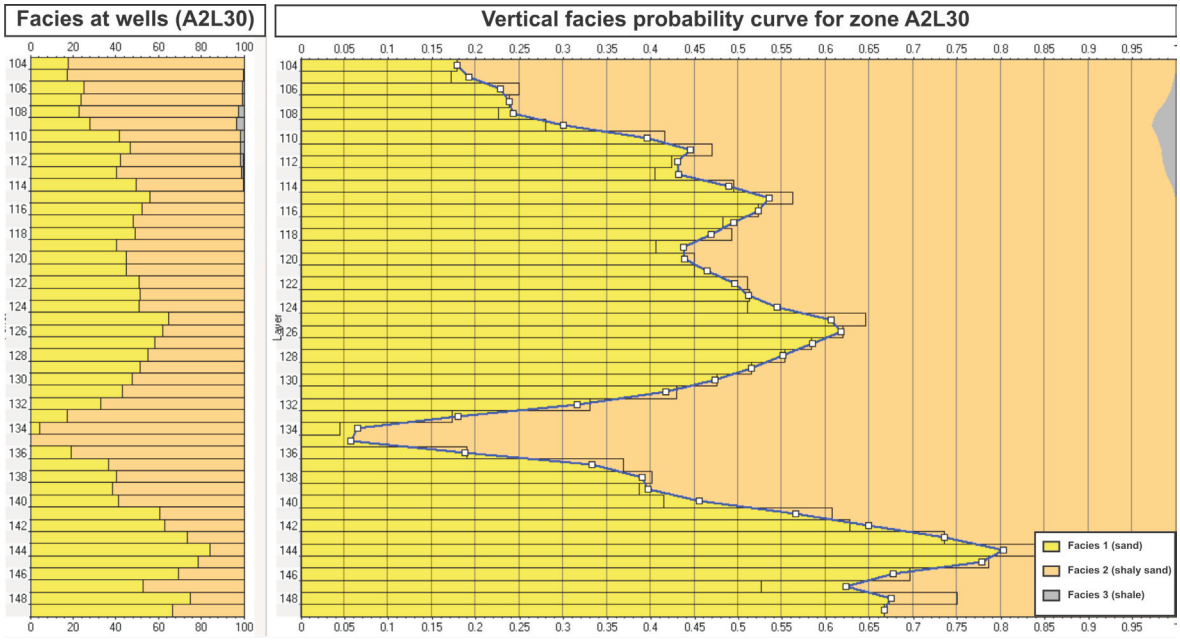

Fig. 47: Vertical probability curve for the interval A2L30

Property distribution in the reservoir intervals

Facies distribution in the reservoir is an iterative process. Settings have to be modified until the point when facies distribution in the reservoir reflects the trends seen in data analysis.

The first step in distributing facies zones is the stochastic distribution of facies groups 2 and 3. This is done in by using a "Sequential Indicator Simulation Process" (Deutsch, et al.). With those two facies groups distributed, facies 1 can be modelled using "Object based Modelling", what means the use of geobodies to distribute the facies in the geologic model. The used geobodies in this case are adaptive channels. The geometry of the geobodies can be defined with following settings:

- Channel width
- Channel thickness
- Sinuosity

This can be set for each reservoir layer separately. In this case settings were kept constant and are based on empirical values from RAG.

The distribution of the facies is done in a few minutes. But how can this process be controlled and validated? This is done by statistics. The ratio from Facies 1 to Facies 2 to Facies 3 can be defined according the calculated facies log. This ratio must remain as constant as possible in the upscaled cells and in the 3D volume of the reservoir model. Otherwise one facies zone is overestimated what will result in misinterpretation and a wrong porosity distribution. The statistic is shown for every reservoir zone and the entire model in Fig. 48. The ratio of facies zone 2 and 3 is not fitting in the entire model. This is a consequence of the barrier layers that were artificially set to facies zone 3, therefore zone 2 is underestimated and zone 3 is overestimated.

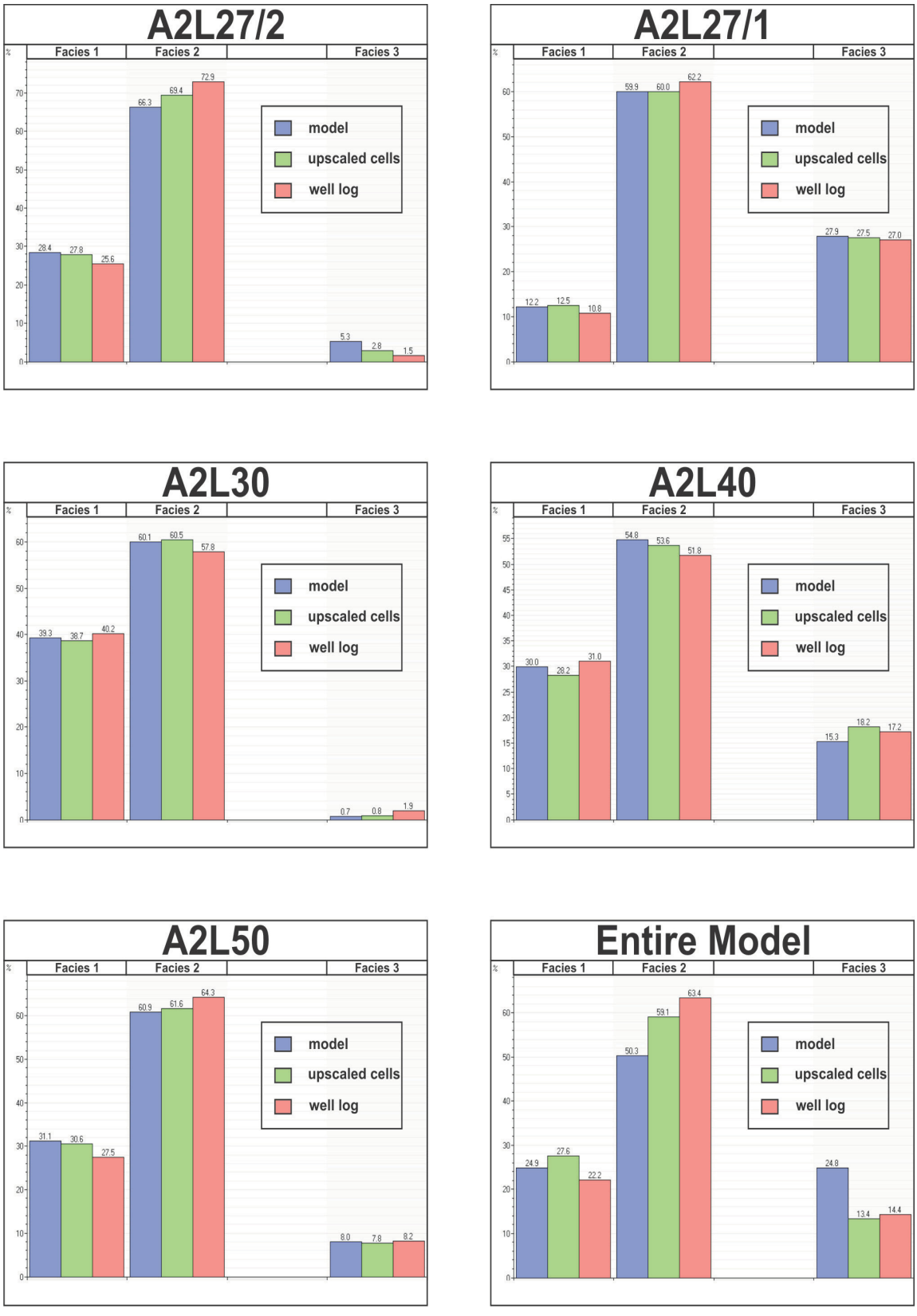

Fig. 48: Statistics for the every reservoir interval and the entire model

The distribution of porosity values is a crucial step in modelling a reservoir concerning the volume calculation of hydrocarbons in place. It is based on the facies distribution within the reservoir. For each facies group defined a porosity range is given and distributed using a Sequential Gaussian Simulation Process (Deutsch, et al.):

- Facies 1: 7-21 %
- Facies 2: 2-7 %
- Facies 3: 0 %

The ranges are based on the calculated porosity log for Facies 1 and estimated for Facies 2, because no porosity log is available. Facies 3 is a non reservoir zone and therefore porosity was set to 0%.

As the porosity is based on the facies zones, the geometry of the geobodies should still be visible in porosity distribution (Fig. 49):

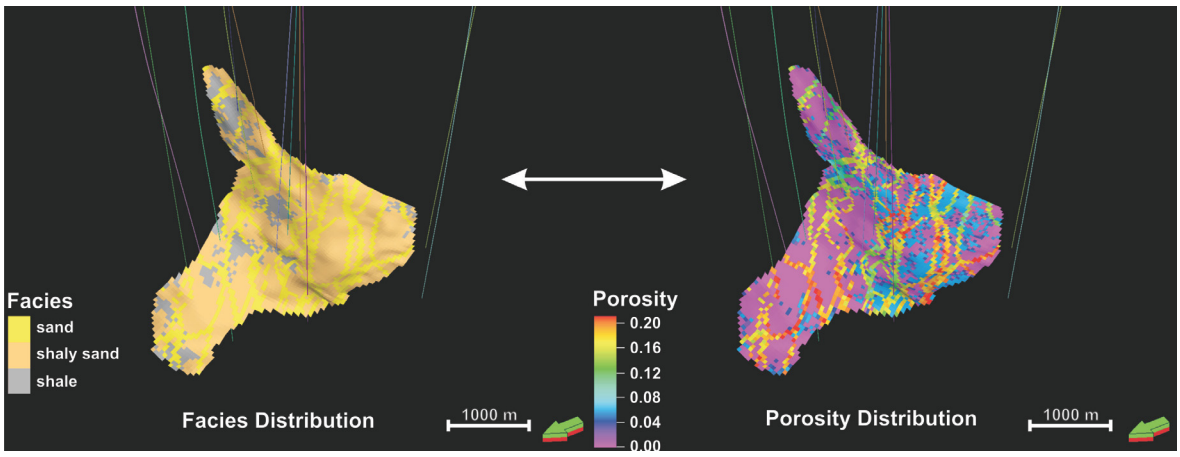

Fig. 49: Comparison of facies and porosity distribution in the reservoir

The final step in modelling a reservoir is to calculate hydrocarbon volumes in place. This was done, but the results are not reported here because of confidentiality reasons. In any case, the results showed an excellent fit with volumes that were estimated by RAG using pressure data.

Conclusion

The Lauterbach Gas Field is complex in its structural and sedimentological framework. The characterisation of the reservoir requires the detailed evaluation of geophysical data as well as information from literature.

The first and most important step on the way to a representative geologic model is to get an overview on the key elements of basin evaluation and how they can be identified in the geophysical data that forms the base of the interpretation. In the Lauterbach Basin those key factors are the synsedimentary deformation that governs the morphology of the accommodation space and the turbiditic sedimentary environment. Latter one is characterised by rapid facies change and a large number of erosive events. Above the base of the Lauterbach basin that is defined by a regional erosive event, five productive sand layers were deposited that vary in areal extend and thickness. Pressure data from productive wells indicate at least some communication between the reservoir units. With bed thickness in the range or smaller than seismic resolution, amplitude variations are a direct indication of bed thickness and therefore are a valuable assist in defining the geometries of the reservoir layers.

For the geologic modelling process, the environment of deposition has to be taken into account. Based on the work of Covault (2009) and core data, a turbidite system described by Mutti (1985) forms the base for the facies model of the Lauterbach Basin. This turbidite system is characterized by small, sand prone channels with fine grained levees that punctuate background sedimentation, resulting in a complex reservoir archicteture. Three facies zones were defined, based on net intervals of the wells and the gamma log to fullfill the requirements of the turbidite model. The distribution of the facies zones in the geologic model was achieved by the use of object based modelling that allows the incorporation of geobodies. In this case adaptive channels were the element of choice. To every facies zone a porosity range was defined, based on porosity data provided by RAG.

For the purpose of on-/off switchable communication paths between the productive reservoir zones, the intervals between were modelled as barrier layers to which a range of porosity values can be assigned.

The last step that would complete the workflow is the calculation of hydrocarbon volume in place. This data is top secret but the fit with volumes calculated from pressure data is excellent.

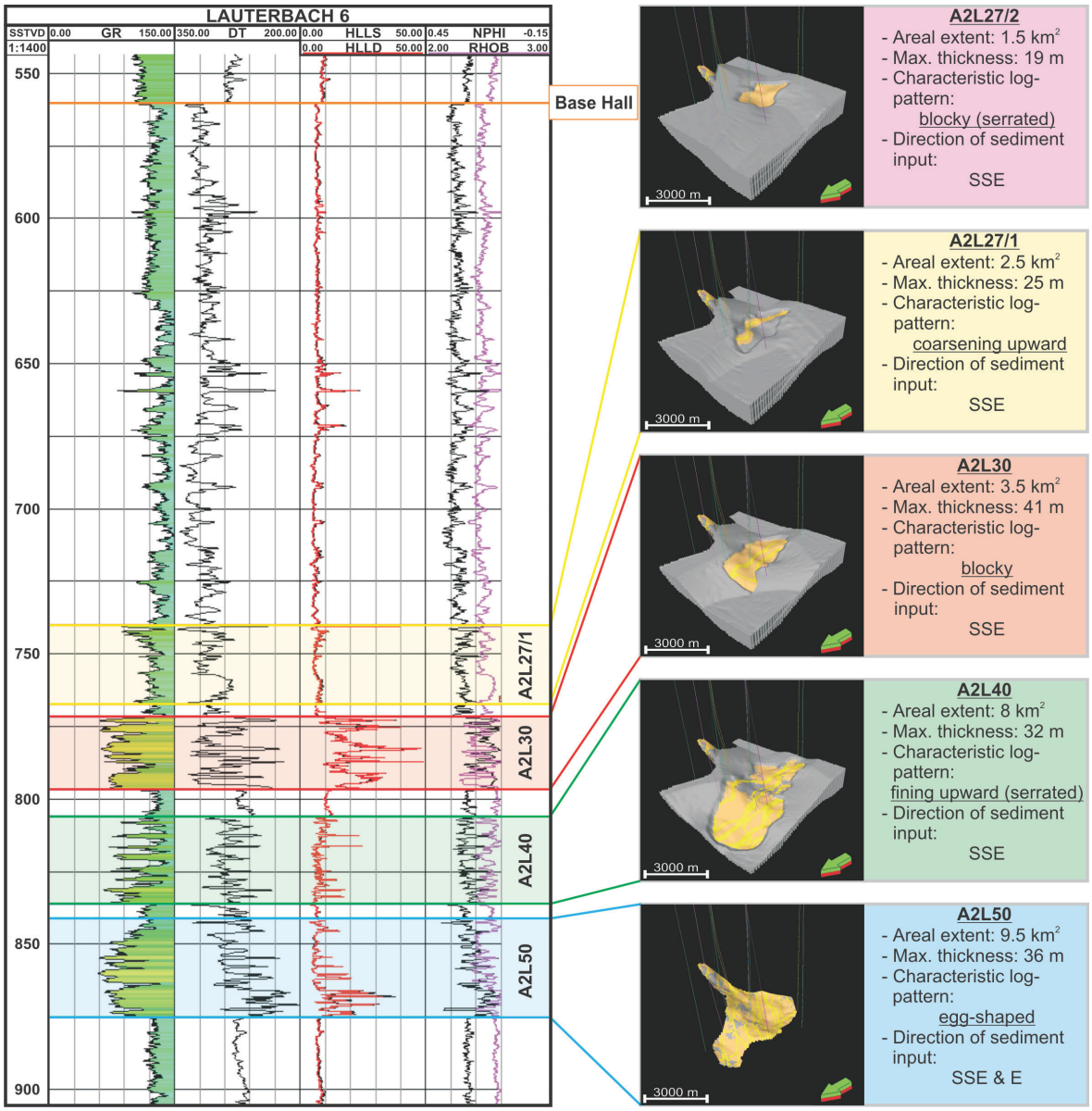

Fig. 50: Architecture of the Lauterbach Gas Field, with 3D pictures of the modelled reservoir layers. Barrier layers are shown in grey colour in the 3D pictures.

The workflow and modelling technique discussed in this thesis led to good results, not only in terms of reservoir engineering but also in terms of geological detail of the model. The most important thing is however to still be aware of the fact that the model based on geostatistical distributions and probabilities that differs from reality.

References

Bachmann, G. H., Müller, M. and Weggen, K. 1986. Evolution of the Molasse Basin (Germany, Switzerland). *Tectonophysics.* 1986, 137, pp. 77-92.

Butler, R. W. H. 1982. The terminology of structures in thrust belts. *Journal of Structural Geology.* 1982, Bd. 3, 4, S. 239-245.

Chadwick, R. A., et al. 2004. 4D Seismic Imaging of an Injected CO2 Plume at the Sleipner Field, Central North Sea. *Memoirs, Geological Society.* 2004, 29, S. 311-320.

Covault, J. A., et al. 2009. Turbidite-reservoir architecture in complex foredeep-margin and wedge-top depocenters, Tertiary Molasse foreland basin system, Austria. *Marine and Petroleum Geology.* 2009, 26, S. 379-396.

Dade, W. B. und Huppert, H. E. 1994. Predicting the geometry of channelized deep-sea turbidites. *Geology.* 1994, 22, S. 645-648.

De Ruig, M. J. und Hubbard, S. M. 2006. Seismic facies and reservoir characteristics of a deep-marine channel belt in the Molasse foreland basin, Puchkirchen Formation, Austria. *AAPG Bulletin.* 2006, Bd. 5, 90, S. 735-752.

DeCelles, P. G. und Giles, K. A. 1996. Foreland basin systems. *Basin Research.* 1996, 8, S. 105-123.

Deutsch, C. und Journel, A. Geostatistical Software Library. [Online] [Zitat vom: 13. 9 2010.] http://www.gslib.com/.

Gochioco, L. M. 1991. Tuning effect and interference reflections from thin beds and coal seams. *Geophysics.* 1991, Bd. 8, 56, S. 1288-1295.

Hubbard, S. M., De Ruig, M. J. und Graham, S. A. 2009. Confined channel-levee complex development in an elongate depo-center: Deep-water Tertiary strata of the Austrian Molasse basin. *Marine and Petroleum Geology.* 2009, 26, S. 85-112.

Kollmann, K. 1977. Die Öl- und Gasexploration in der Molassezone Oberösterreichs und Salzburgs aus regional-geologischer Sicht. *Erdöl-Erdgas-Zeitschrift.* 1977, 93, S. 36-49.

Malzer, O., et al. 1993. Die Molassezone und deren Untergrund. *Erdöl und Erdgas in Österreich.* Horn : Naturhistorisches Museum Wien und F. Berger, 1993, pp. 281-358.

Morley, C. K. und Leong, L. C. 2008. Evolution of deep-water synkinematic sedimentation in a piggyback basin, determined from three-dimensional seismic reflection data. *Geosphere.* 2008, 4, S. 939-962.

Mutti, E. 1985. Turbidite systems and their relations to depositional sequences. [Buchverf.] G. G. Zuffa. *Provenance of Arenites.* Amsterdam : Reidel, 1985, S. 65-93.

Ori, G. G. and Friend, P. F. 1984. Sedimentary basins formed and carried piggyback on active thrust sheets. *Geology.* 1984, 12, pp. 475-478.

Robertson, J. D. und Nogami, H. H. 1984. Complex seismic trace analysis of thin beds. *Geophysics.* 1984, Bd. 4, 49, S. 344-352.

Sachsenhofer, R. F., et al. 2010. Deposition, Erosion and Hydrocarbon Source Potential of the Oligocene Eggerding Formation (Molasse Basin, Austria). *Austrian Journal of Earth Sciences.* 2010, 103/1, S. 76-99.

Schulz, H.-M., et al. 2002. The origin of hydrocarbon source rocks in the Austrian Molasse Basin (Eocene - Oligocene transition). *Marine and Petroleum Geology.* 2002, 19, S. 683-709.

Shanmugam, G. 2002. Ten turbidite myths. *Earth-Sience Reviews.* 2002, 58, S. 311-341.

Sissingh, W. 1997. Tectonostratigraphy of the North Alpine Foreland Basin: correlation of Tertiary depositional cycles and orogenic phases. *Tectonophysics.* 1997, Vol. 282, pp. 223-256.

Steininger, F. F., et al. 1986. Tertiary sedimentary history and tectonic evolution of the Eastern Alpine Foredeep. *Giornale di Geologia.* 1986, 48, pp. 285-297.

Wagner, L. R. 1996. Stratigraphy and hydrocarbons in the Upper Austrian Molasse Foredeep (active margin). [book auth.] G. Wessely and W. Liebl. *Oil and Gas in Alpidic Thrustbelts and Basins of Central and Eastern Europe.* s.l. : EAGE Special Publication, 1996, Vol. 5, pp. 217-235.

Wagner, L. R. 1998. Tectono-stratigraphy and hydrocarbons in the Molasse Foredeep of Salzburg, Upper and Lower Austria. [book auth.] A. Mascle, et al. *Cenozoic Foreland Basins of Western Europe.* s.l. : Geological Society, 1998, Vol. 134, pp. 339-369.

Zoetemeijer, R., et al. 1993. Modelling of piggyback-basin stratigraphy: record of tectonic evolution. *Tectonophysics.* 1993, 226, S. 253-269.

List of Figures